



Universidad de Valladolid



**ESCUELA DE INGENIERÍAS
INDUSTRIALES**

UNIVERSIDAD DE VALLADOLID

ESCUELA DE INGENIERIAS INDUSTRIALES

Grado en Ingeniería Electrónica Industrial y Automática

**Survey on individual components for a 5 GHz receiver system
using 130 nm CMOS technology**

Autor:

Noriega del Rivero, Sergio

Francisco Javier Rey Martínez

Technische Universität Dresden

Valladolid, JUNIO 2020.

TFG REALIZADO EN PROGRAMA DE INTERCAMBIO

TÍTULO: Survey on individual components for a 5 GHz receiver system using 130 nm CMOS technology

ALUMNO: NORIEGA DEL RIVERO, SERGIO

FECHA: 11/06/2020

CENTRO: FAKULTAT ELEKTROTECHNIK UND INFORMATIONSTECHNIK

UNIVERSIDAD: TECHNISCHE UNIVERSITÄT DRESDEN

TUTOR: PROF. DR-ING. HABIL. MICHAEL SCHRÖTER

Abstract

The intention of this thesis is to gather information from an overview point about the different types of components used in a 5 GHz receiver using CMOS technology. A review of each of the components that form the system has been made, highlighting different types of configurations, figure of merits and parameters. A summary table is shown at the end of each section, comparing many designs that have been presented over the years at international conferences of the IEEE.

Keywords: CMOS, Receiver, Amplifier, Mixer, Oscillator.

Resumen

La intención de esta tesis es recopilar información desde un punto de vista general sobre los diferentes tipos de componentes utilizados en un receptor de señales a 5 GHz utilizando tecnología CMOS. Se ha realizado una descripción y análisis de cada uno de los componentes que forman el sistema, destacando diferentes tipos de configuraciones, figuras de mérito y otros parámetros. Se muestra una tabla resumen al final de cada sección, comparando algunos diseños que se han ido presentando a lo largo de los años en conferencias internacionales de la IEEE.

Palabras clave: CMOS, Receptor, Amplificador, Mezclador, Oscilador.

TECHNISCHE UNIVERSITÄT DRESDEN
FAKULTÄT ELEKTROTECHNIK UND
INFORMATIONSTECHNIK

Institute for Fundamentals of Electrical Engineering and
Electronics (IEE)
Chair of Electronic Components
and Integrated Circuits

BACHELOR THESIS

on the subject
**Survey on individual components for a 5 GHz receiver system
using 130 nm CMOS technology.**

Presented by

Sergio Noriega del Rivero

Matriculation Number: 4920837

Supervisor 1:
Supervisor 2:

Dr. Ing. Anindya Mukherjee
Prof. Dr-Ing. habil. Michael Schröter

June 2020

Copyright © 2020 by Sergio Noriega del Rivero.
All rights reserved

To my parents and brother

Abstract

The intention of this thesis is to gather information from an overview point about the different types of components used in a 5 GHz receiver using CMOS technology. A review of each of the components that form the system has been made, highlighting different types of configurations, figure of merits and parameters. A summary table is shown at the end of each section, comparing many designs that have been presented over the years at international conferences of the IEEE.

Contents

<i>Abstract</i>	<i>i</i>
<i>Contents</i>	<i>ii</i>
<i>List of Figures</i>	<i>iv</i>
<i>List of Tables</i>	<i>vi</i>
<i>Abbreviations</i>	<i>vii</i>
1. Background	1
1.1 Metal-Oxide-Semiconductor Field-Effect Transistor	1
1.2 Complementary metal-oxide-semiconductor technology	2
2. Transmitter and receiver systems	5
2.1 Introduction	5
2.2 CMOS Technology in Transceiver Systems	6
2.3 Noise and Linearity in CMOS Technology	6
2.4 1dB Compression Point (P1dB)	7
2.5 Intercept Point	7
2.6 Receiver Configurations	9
2.6.1 The Super-Heterodyne Architecture	9
2.6.2 The Zero-If and Low-If Architecture	10
3. Literature review of components in a receiver system with CMOS technology	13
3.1 Low Noise Amplifier (LNA)	13
3.1.1 Background	13
3.1.2 Characteristics	13
3.1.3 Design Configurations	15
3.1.4 LNA Applications for 5 GHz	25
3.2 Up and Down Conversion Mixer	30
3.2.1 Background	30
3.2.2 Conversion gain and conversion loss	31
3.2.3 Design configurations	32
3.2.4 Applications	34

3.3	Oscillator	37
3.3.1	Introduction and General Background	37
3.3.2	Ideal LC Tank	38
3.3.3	Oscillator parameters	40
3.3.4	Voltage Controlled Oscillator (VCO)	43
3.4	Power amplifier (PA)	51
3.4.1	Background	51
3.4.2	Basic PA Parameters and Characteristics.....	51
3.4.3	Amplification-mode PA	53
3.4.4	Switching-mode PAs.....	59
3.4.5	Applications and Figure of Merits (FoMs).....	62
4.	Conclusion	66
5.	References	68

List of Figures

Figure 1. a) MOS structure. Symbols of MOS b) with bulk terminal c) without bulk terminal [1].	1
Figure 2. Example of CMOS digital circuit. NMOS and PMOS connected in parallel.	2
Figure 3. Fabrication of a CMOS Transistor [4].	3
Figure 4. Common Logic Gate using pull-up and pull-down blocks.	3
Figure 5. Definition of P1dB.	7
Figure 6. Definition of third order intercept point.	8
Figure 7. Super-heterodyne receiver.	9
Figure 8. Generic Zero/Low IF receiver.	10
Figure 9. Techniques to get resistive term in the input impedance of an LNA [11].	14
Figure 10. Common gate CMOS LNA [24].	16
Figure 11. NMOS common-source amplifier.	18
Figure 12. Common-source CMOS LNA with input matching [32].	18
Figure 13. CS LNA with an inductive degeneration [38].	19
Figure 14. Cascode topology with source degeneration [24].	20
Figure 15. Amplifier with capacitance between input and output.	22
Figure 16. Effective capacitance circuit.	22
Figure 17. Distributed amplifier [46].	22
Figure 18. Conventional differential amplifier.	23
Figure 19. Differential capacitive cross coupled low-noise amplifier configuration [45].	24
Figure 20. Resistive current reuse amplifier [53].	25
Figure 21. Frequency mixer symbol a) Up-conversion b) Down-conversion.	30
Figure 22. Two input signals mixed and the output as the result.	31
Figure 23. CMOS voltage mixer [72].	32
Figure 24. Gilbert cell mixer topology [6].	33
Figure 25. Double-balanced Gilbert cell mixer [6].	33
Figure 26. Block diagram with positive feedback [8].	37
Figure 27. Most basic LC oscillator.	38
Figure 28. Oscillation of the basic LC oscillator a) with no feedback b) with feedback and energy supply.	39
Figure 29. LC tank a) parallel b) series.	39
Figure 30. Possible parallel LC tank solutions.	40
Figure 31. Possible interferences caused by phase noise [8].	41
Figure 32. Frequency spectrum of a) ideal oscillator b) real oscillator [95].	42
Figure 33. Amplitude and phase noise in time domain [8].	43
Figure 34. Triangular waveform from a relaxation oscillator.	44
Figure 35. CMOS single ended Colpitts oscillator [97].	45
Figure 36. Cross-coupled VCO using CMOS [5].	46
Figure 37. 3-stages ring-VCO [98].	47
Figure 38. Three stages oscillator [3].	47
Figure 39. Graphics representing linearity of a PA: a) AM-to-AM b) AM-to-PM [118].	52

Figure 40. Power amplifiers divided by classes [121].	53
Figure 41. Single-stage Class A PA [122].	54
Figure 42. Drain voltage and current waveforms for Class A PA [119].	54
Figure 43. Differential Class B PA [117].	55
Figure 44. Drain voltage and current waveforms for Class B PA [119].	55
Figure 45. Pull-push CMOS Class-B PA.	56
Figure 46. Crossover distortion for Class-B PA [125].	56
Figure 47. Drain voltage and current waveforms for Class-C [119].	57
Figure 48. Conduction mode in different classes of amplification-mode PA [114].	58
Figure 49. Class D PA [122].	59
Figure 50. Class E PA [122].	60
Figure 51. Class F PA [122].	61

List of Tables

Table 1. 5GHz LNA comparison with 130 nm CMOS technology.	27
Table 2. 5GHz LNA comparison with 90, 180 and 250 nm CMOS technology.	28
Table 3. Comparison table of reported 5 GHz low-voltage CMOS UP-conversion mixers.	35
Table 4. Comparison table of reported 5 GHz low-voltage CMOS DOWN-conversion mixers.	35
Table 5. Comparison table of reported 130 nm CMOS VCOs.....	49
Table 6. Comparison table of reported 90, 180 and 250 nm CMOS VCOs.....	49
Table 7. Summary table of the theoretical characteristics of the amplification-mode PA.....	58
Table 8. CMOS Amplification-Mode Power Amplifier comparison table.	63
Table 9. CMOS Switching-Mode Power Amplifier comparison table.	64

Abbreviations

ACLR	Adjacent Channel Leakage Ratio
ACPR	Adjacent Channel Power Ratio
BJT	Bipolar Junction Transistor
CG	Common gate
CMOS	Complementary Metal-Oxide-Silicon
CS	Common source
DC	Direct Current
DE	Drain Efficiency
ESD	Electrostatic discharge
EVM	Error Vector Magnitude
FET	Field-Effect Transistor
FoM	Figure of Merit
GaAs	Gallium-Arsenide
HBT	Heterojunction Bipolar Transistor
IC	Integrated Circuit
IMN	Input Matching Network
ITRS	International Terrestrial Reference System
LNA	Low-noise Amplifier
LO	Local Oscillator
MOS	Metal-Oxide-Semiconductor
MOSFET	Metal-Oxide-Semiconductor Field Effect Transistor
NMOS	N-channel Metal-Oxide-Semiconductor
OMN	Output Matching Network
PA	Power Amplifier
PAE	Power-added efficiency

PMOS	P-channel Metal-Oxide-Semiconductor
RF	Radio-Frequency
RX	Receiver
SNR	Signal-to-noise Ratio
SoC	System on chip
TX	Transmitter
VCO	Voltage-Controlled Oscillator
WLAN	Wireless Local Area Network

CHAPTER 1

1. Background

1.1 Metal-Oxide-Semiconductor Field-Effect Transistor

Transistors are the basic devices for creating electronic circuits. The main difference between active devices such as transistors, and passive elements such as resistors, capacitors, inductors and diodes, is that the current and voltage characteristics of transistors vary with the voltage or current on a control terminal. There are two types of transistors: bipolar and field-effect transistors, known as FET. FET can be divided in two groups: junction field-effect transistors (JFETs) and metal-oxide-semiconductor field-effect transistors (MOSFETs). Like BJTs, MOSFETs have three terminals: gate, source and drain. A fourth terminal, called bulk or body (B), can be labelled as shown in Figure 1b) or not drawn in Figure 1c) [1].

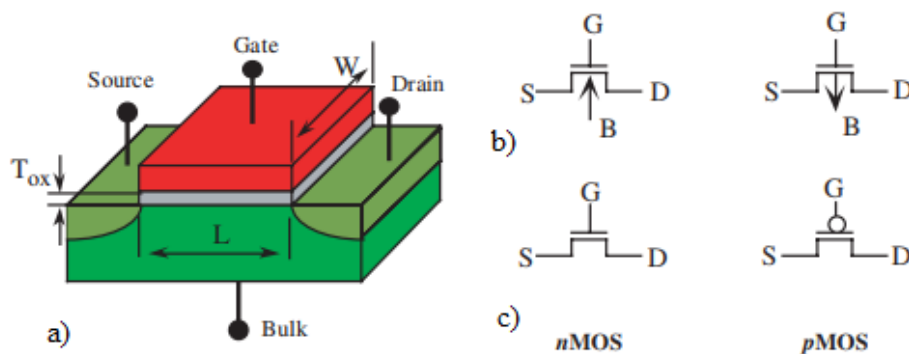


Figure 1. a) MOS structure. Symbols of MOS b) with bulk terminal c) without bulk terminal [1].

MOSFETs are unipolar devices where the current transportation is carried out by electrons or holes. While BJTs are fed by a large base current, MOSFET can be driven with a lower current due to the high input impedance. Electrical circuits which require low voltage supplies are typically implemented in MOSFET [2].

Many applications need MOSFETs to operate as switches, like Class D power amplifiers. When the gate has a high voltage, the transistor closes, connecting drain and source and letting the current to flow. When the gate does not have enough voltage, the transistor acts as an open circuit. An ideal transistor should switch between ON and OFF states with no delay. In practice, this is not possible. The delay, and so other parameters such as threshold voltage or doping levels, are determined by fabrication processes [1], [2].

1.2 Complementary metal-oxide-semiconductor technology

Complementary Metal-Oxide-Semiconductor (CMOS) technology was introduced in the mid-1960s, initiating a revolution in the semiconductor industry. It is a type of metal-oxide-semiconductor field-effect transistor (MOSFET) which consists in a combination of two transistors, one NMOS and other PMOS. In most CMOS technologies, NMOS transistors present a better performance than the PMOS since NMOS have higher current drive and transconductance. It is commonly used in integrated circuit fabrication processes. Most integrated circuits such as microprocessors, microcontrollers, or memories like RAM, ROM or EEPROM use CMOS technology.

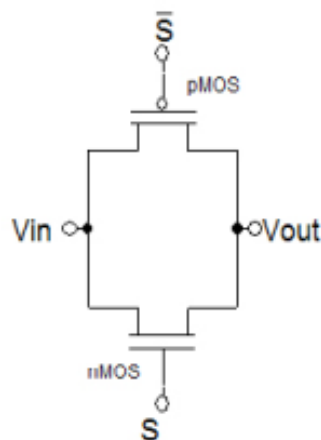


Figure 2. Example of CMOS digital circuit. NMOS and PMOS connected in parallel.

The most remarkable advantage of CMOS technology is that the static power dissipation is practically negligible. Power is dissipated only when the circuit operates as a switch. This characteristic, plus the capability of reducing the size of the circuits more easily, are two great advantages compared to bipolar or GaAs technologies [3]. CMOS technology offers considerable high speed and low power dissipation, but it presents high noise margins [4]. Noise Figure in CMOS technology will be discussed in Section 2.3.

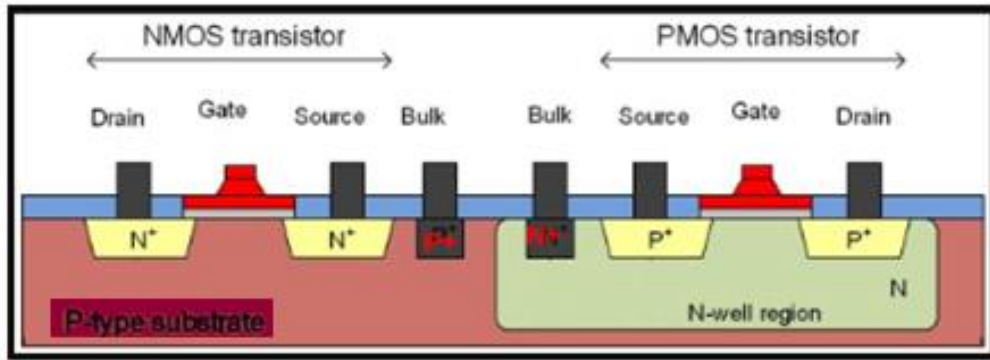


Figure 3. Fabrication of a CMOS Transistor [4].

Complementary Metal-Oxide-Semiconductor transistor consists of P-channel MOS (PMOS) and N-channel MOS (NMOS). NMOS transistor is fabricated on a p-type substrate. The source and drain are formed with two doped n regions. When the voltage between gate and source, V_{GS} , is higher than the threshold voltage (V_{th}), then NMOS will conduct. PMOS operates in the opposite way. PMOS is built on a n-type substrate with p-type source and drain diffused on it. In this case, when V_{GS} is lower than V_{th} , the transistor will conduct. NMOS are faster than PMOS due to the carriers in NMOS being electrons instead of holes. However, PMOS devices present less noise than NMOS devices [5].

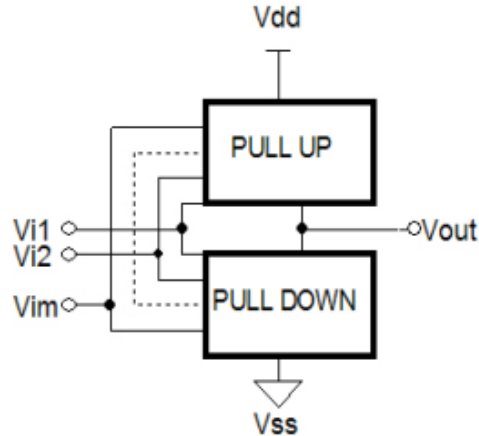


Figure 4. Common Logic Gate using pull-up and pull-down blocks.

CMOS technology applied in digital devices are formed by the connection of two complementary blocks with same inputs and outputs, pull-up and pull-down networks. Pull-up is formed only by PMOS transistors connected to V_{DD} . Transistors in the pull-up block will transmit the high logic state. Pull-down block is formed by NMOS transistors and it is connected to ground (V_{SS}). It will transmit the low logic state. Thus, the same signal will turn on a transistor of one type and turn off the other. In this way, a wide variety of logic gates can be achieved such as inverters, AND, NAND or NOR gates, among others. However, in this report we will be focused on the analog design using CMOS.

CHAPTER 2

2. Transmitter and receiver systems

At first, an introduction about transmission and receiver systems is presented. Different components used in a 5 GHz receiver system are discussed in this report. Main components used in a receiver are low-noise amplifiers (LNAs), mixer, voltage-controlled oscillators (VCOs) and power amplifiers (PAs).

2.1 Introduction

Transmission and receiver (or transceiver) systems are devices which transmit and receive electromagnetic signals. The signals in which information travels are transmitted by using high frequency. Transceiver systems, like a common radio are characterized by their carrier frequency. Usually a carrier frequency for a radio is 900MHz or 5 GHz [6], and generally, the higher the carrier frequency, the better directivity, but the more complex circuit design.

Most radio receiver systems use the same basic architecture although there are varieties on the configuration [7]. These different configurations will be discussed in this report. Main functions of a receiver system are capturing the radio waves with an antenna, processing all the waves and extracting only the desired waves which vibrate at the wanted frequency. An important aspect to consider is the strong attenuation that signals can suffer during air transmission. For this reason, RF signals must be amplified and recovered [8].

Receivers should not be turn off completely, otherwise, signals cannot be received when a transmitter is emitting data. Receivers shall detect whenever a transmitter requests an active communication. That is the reason why two different working modes are found in the receivers. If the receiver is not active, then it must work in the stand-by mode, in which DC power consumption should be much less than in the active mode. Due to this reason, DC power consumption is one of the most important parameters when designing a receiver. On the other hand, some transmitter functions are modulation, frequency conversion and power amplification. Unlike receivers, transmitters can be completely switched off for power saving. These only need to be in the active mode when data wants to be transmitted. Normally, the power consumption of transceivers is measured by its transmitter power consumption rather than by its receiver's. This is because transmitters need a high output power to emit data and that leads to a high DC power consumption [8].

2.2 CMOS Technology in Transceiver Systems

Over the years, the integration of more complex circuits into smaller chips has become a reality. The integration of circuits using CMOS technology went low cost and drives the improvement of modern radio frequency integrated circuit designs. It is now possible to use this technology in transceiver systems, such as 5 GHz wireless LAN systems. Designers have been studying how to implement improvements to the main features of the various IC building blocks which make up a device on smaller and smaller chips.

CMOS processes are usually preferable in comparison with other processes, like bipolar or GaAs, because of its lower cost and better integration with digital signal processing (DSP) chips. In addition, the size of CMOS devices has been more easily shrunken than other technologies. However, limitations in noise and linearity has become a challenge for designers since other processes like GaAs present better performance in these aspects [6].

2.3 Noise and Linearity in CMOS Technology

The Noise Figure (NF) also called *noise factor*, is the decrease in the signal-to-noise ratio (SNR) as a signal passes through a system network [9]. The signal-to-noise ratio is an important figure of merit (FoM) in receivers. It is a measure which compares the level of the wanted signal to the level of the noise. Thus, a low noise figure means the system is working with very little level of added noise.

This parameter is used to make comparisons between different devices by measuring the added noise produced by these systems. With the noise figure, system's sensitivity can be calculated from its bandwidth. In case of a receiver, the sensitivity indicates what is the weakest signal that the receiver will be able to identify and process [9], [10]. The lower the noise figure, the better the sensitivity. Some authors have studied how the use of MOSFET transistors normally present more noise figure than circuits which use bipolar transistors. However, the use of CMOS technology has improved the performance in this aspect in recent years, obtaining noise figures close to HBT or bipolar circuits [6]. The way of improving the NF of CMOS technology is by applying noise figure optimization techniques described in [11]. Noise figure optimization techniques will be discussed in the next sections.

Linearity specifies the capacity of a device to manage large signals. Intermodulation can appear while using large signals which drive to an inefficient circuit and bad performance. CMOS circuits need linearization techniques to improve linearity and to try getting as good performance as GaAs circuits.

2.4 1dB Compression Point (P1dB)

Related to linearity limitations of CMOS technology, there is a parameter which describes the tolerance to desensitization of a circuit called the *1 dB compression point*. This parameter describes the output power level at which the gain decreases 1 dB from its constant value. When an amplifier reaches the P1dB it goes into compression and behaves more in non-linear way producing harmonics, distortion and intermodulation products.

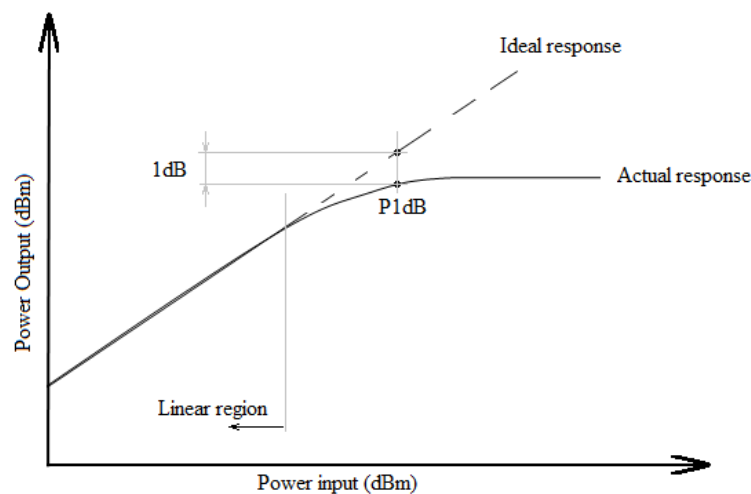


Figure 5. Definition of P1dB.

The 1 dB compression point is one of important figure of merit (FoM) for circuits like low-noise amplifiers, power amplifiers or mixers. In general, CMOS have a lower P1dB which limits the output power for linear operations [6].

2.5 Intercept Point

When a system is non-linear, undesired harmonics may appear. The second, third, and higher harmonics are generally beyond the device's bandwidth so they could be filtered out without any problem. But, on the other side, when a system is working non-linearly, it will also produce a mixing effect of two or more input signals. This mix of frequencies (Intermodulation products) can be within the operating bandwidth of the device and it is difficult to filter them out [12]. Here is where the concept of the intercept point comes into play.

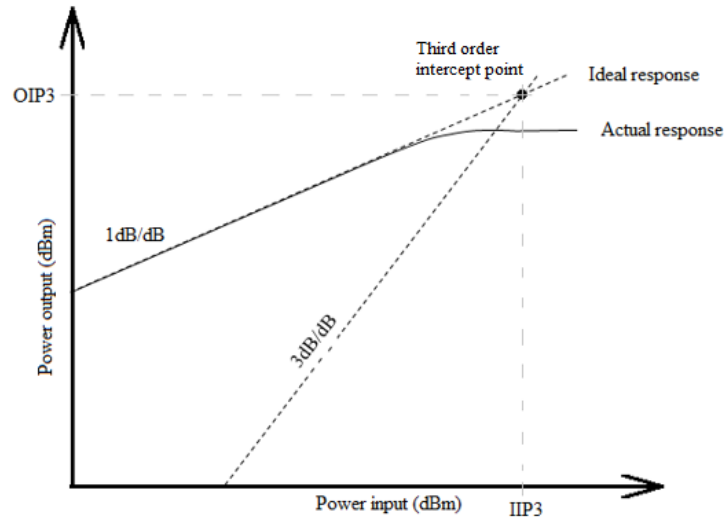


Figure 6. Definition of third order intercept point.

The third intercept point value (IP3) measures how long a signal can be processed by the device before intermodulation distortion (IMD) occurs [12]. This concept describes the linearity of a circuit and is commonly used to indicate the level of intermodulation. It is defined as the point in which linear extrapolation of the fundamental signal and linear extrapolation of the n^{th} order harmonic cross each other. It can be read from the input (IIP3) or output (OIP3) power axis [6]. The third order intercept point (IP3) is shown in Figure 6. Specially, IP3 is a specific figure of merit of nonlinear systems and devices like receivers, transmitters, amplifiers or mixers. The higher the IP3, the smaller the intermodulation signal [6].

The IIP3 is an important parameter when designing a receiver because it gives an idea of how much distortion is produced by our device [12]. The objective when designing a circuit is to achieve the highest IIP3 taking care of power consumption, size or gain. Keeping a high value of IIP3 means the device will be better.

2.6 Receiver Configurations

2.6.1 The Super-Heterodyne Architecture

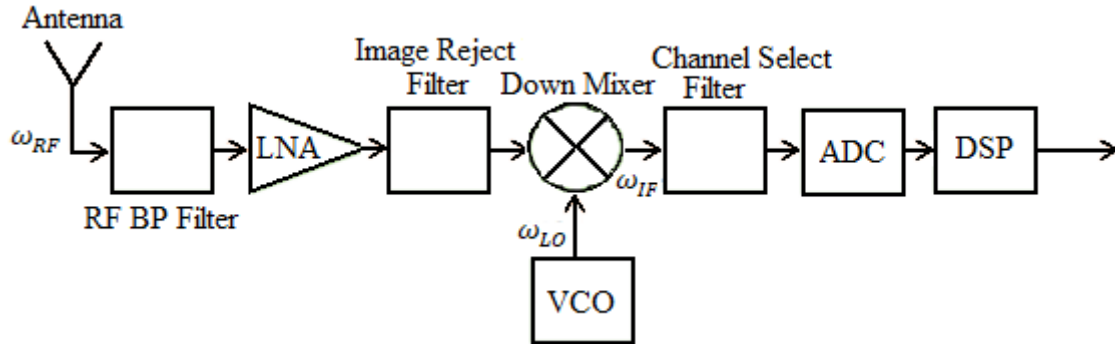


Figure 7. Super-heterodyne receiver.

Conventional super-heterodyne receiver is shown in image above. Main components of a receiver are low-noise amplifiers, mixer, filters, local oscillator and demodulator. This configuration is called super-heterodyne because of the combination of terms “supersonic” and “heterodyne”. It is supersonic, since signal is not audible in the intermediate frequency stage, and heterodyne, because the local oscillator device must work at a different frequency than the received signal [13].

The antenna is connected to the LNA, but it also could be connected to a selective bandpass filter which eliminates possible interferers. Low-noise amplifier improves the weakest channels and send the signal to next block, the mixer. Mixer will get a new output signal frequency from two input signals, RF and LO.

In receivers, it is important to pay attention in filters, especially in image filters. These are in charge of filtering out those frequencies that could be located above and below the LO frequency. If those frequencies are not filtered and they pass through the mixer, there is no way to separate the original signal and the interferer image signal. To solve this problem, an image rejection filter is required to suppress the mirror signal at next frequency,

$$f_{image} = IF_{current} + 2IF_{new} \quad (1)$$

where $IF_{current}$ is the frequency of the current of the signal received and IF_{new} is the frequency signal obtained after the mixer [7]. Is important to pay attention on this issue, otherwise, signals whose frequency is similar to the image frequency could interfered in our desired signal [13]. This means that, if the frequency of an image

signal is less than two times the intermediate frequency, the receiver will pick it up and will convert it to the IF [14]. In addition, the first filter connected before the LNA contributes to filtering image frequency signals. The way of solving image interfering problem is by using high-Q (quality factor) tuned circuits ahead of the mixer. With a higher quality factor, the bandwidth is reduced, so there are fewer frequencies that can interfere with the system. Normally, having higher Qs is difficult and circuit designs become more complicate. Another solution is using a higher IF. With a higher IF, the minimum frequency that can interfere with the system also increases [14]. Thus, it is very difficult to achieve the necessary Q factor. That is the reason why the conversion ratio must be realized in two or more steps, requiring more image filters [7].

2.6.2 The Zero-If and Low-If Architecture

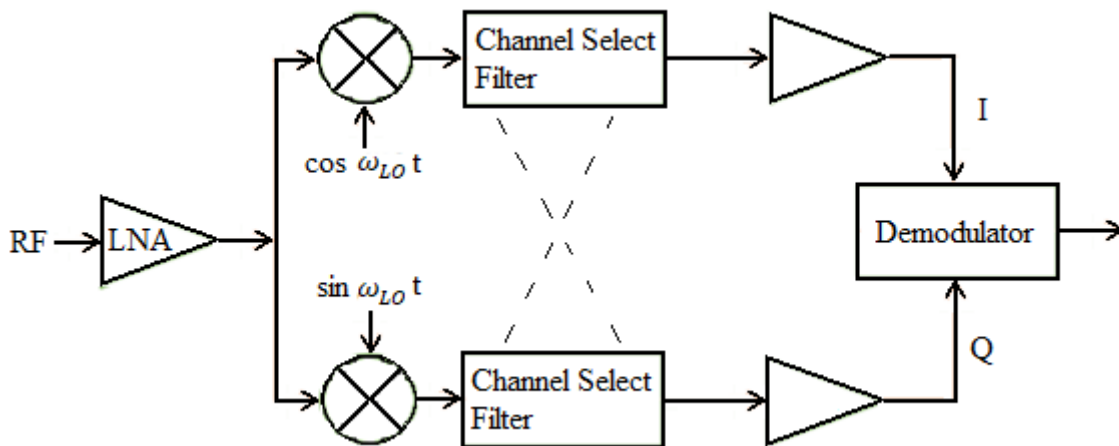


Figure 8. Generic Zero/Low IF receiver.

Figure 8 illustrates both a generic zero and low IF receivers. In these architectures, the main tasks to achieve is amplification, quadrature down conversion, filtering and demodulation [15]. The first step in both architectures is that the signal received by the antenna passes through a band select filter in order to eliminate possible disturbances. In the second step, the signal is divided in to two independent signals and are connected to an RF mixer [7]. Two parallel ways with independent mixers are connected to a common LO signal whose phase shift is 90° . Each path drives a single stage down conversion of the desired signal to the intermediate frequency. In one of the paths there will be an in-phase component (I) and in the other a quadrature component (Q). Here comes the difference between low and zero IF architectures. In the low IF receiver, the RF signal is mixed down to a lower nonzero frequency or

intermediate frequency while in the zero IF receiver, the signal is converted to DC [7].

In the next chapter, the necessary components for implementing a receiver system using CMOS technology will be discussed. Different characteristics of those components will be compared.

CHAPTER 3

3. Literature review of components in a receiver system with CMOS technology

3.1 Low Noise Amplifier (LNA)

3.1.1 Background

A low-noise amplifier is an electronic amplifier that operates with a low input signal and obtains considerable good gain without amplifying possible noise received in the input. It amplifies the signal without adding much noise at its output. A typical amplifier receives the power signal and undesired noise in its input and increase both. In addition, the amplifier itself produces an undesired noise which will make the amplifier's output worse. Hence, there will be too much amplified noise in the output signal. To achieve a better performance, LNAs are necessary to have optimum noise performance while having decent gain.

Thus, in most high-performance radio receivers a receiver system must have an LNA as the first active block. It is typically the first block after the antenna and its design is fundamental for the correct operation of the receiver. It is the one in charge of amplifying the input signals so that the noise produced by following blocks have less impact on the system signal-to-noise ratio (SNR) [16], [17].

Depending on the applications, several circuits with different configurations have been proposed over the years for LNA. The most common designs of CMOS LNA circuits were generated with common gate (CG) or common source (CS) topologies. There are other different configurations, such as cascode stages, used in radio frequencies (RF) [18] which will be discussed in Section 3.1.3.

3.1.2 Characteristics

The two most critical characteristics of an LNA architecture are noise efficiency and power gain. Other parameters, such as DC power consumption, stability or voltage supply can also affect LNA's performance.

Getting minimum noise figure (NF) and maximum power gain hardly happen at the same impedance state. That is why a correct input matching network is required in order to improve both parameters [17]. One of the most significant aspects of CMOS technology is that it can provide a good minimal LNA noise (NF_{min}) with also a considerable good usable power gain at the same time. Having a good noise figure is possible using optimum noise matching. On the other hand, having

maximum power gain is possible using a correct impedance matching known as conjugate matching. Hence, these two different configurations are opposite ways of matching the transmission line, so it would not be possible to obtain them simultaneously without CMOS technology [19], [20]. T. Yao et. al [19] designed a 60 GHz power and low-noise amplifier using 90 nm CMOS technology. In this paper, T. Yao et. al measured the optimal minimum noise figure (NF_{min}), which occurs at 0.15 mA/ μm and was considerably close to the peak (f_{max}) current density which occurs at 0.2 mA/ μm .

Favourably, as we have seen, one important advantage of CMOS technology is that minimum noise figure and maximum power gain are very close together, so it is easier to get a considerable good noise performance [19]. It depends on the width of the CMOS transistor. Input and noise matching were studied by H. Song et. al in 2008 [21] where it is explained how to choose components to satisfy the optimum matching conditions using the Smith Chart.

The input impedance of a low-noise amplifier must have a resistive term in order to get the best power gain matching. There are many different techniques which can provide the necessary resistive term in the input impedance of an LNA and they are shown in Figure 9 [11].

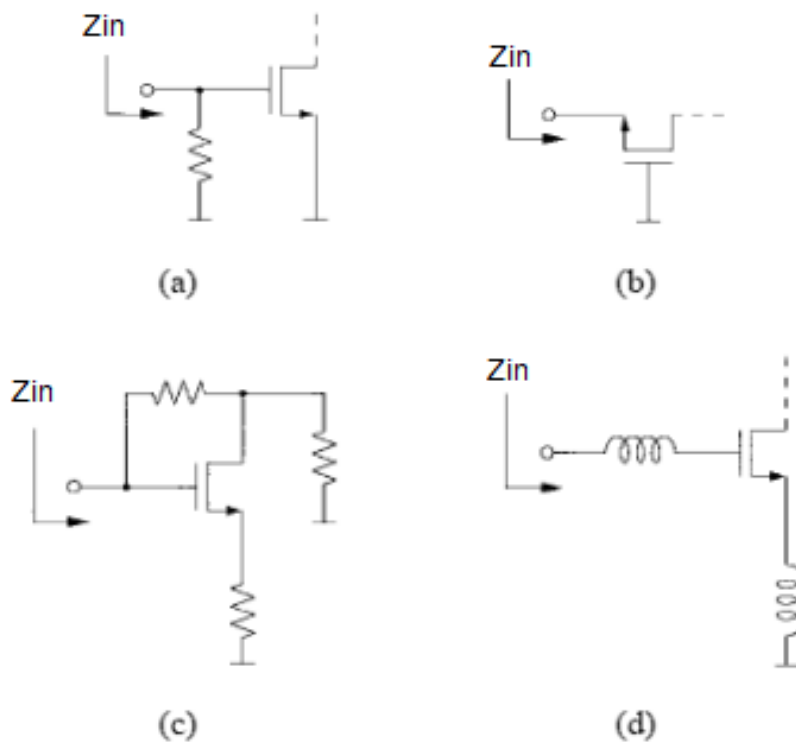


Figure 9. Techniques to get resistive term in the input impedance of an LNA [11].

First method shown in Figure 9.a) uses a resistive termination of the input to provide the conjugate matching of 50Ω impedance. This resistor adds noise to the amplifier hence it has a negative effect on noise figure of the LNA. Suppose that an amplifier with no resistive term presents a 6dB noise figure. If the resistor is added, noise figure will increase to 11.5dB. This increase in noise figure can be explained by the next two effects. First of all, the resistor has his own noise which is added to the output noise. Second, the input is attenuated because of the resistor, which makes the total output noise higher. Degradation of noise figure is the main reason why designers do not usually use this method in their designs [11].

Second technique shown in Figure 9.b) uses the source or emitter of a common-gate or common-base stage as the input termination. Assuming matched conditions, CMOS amplifiers drives a noise factor of 2.2 dB evaluated at 290K temperature as shown in [11] paper.

Third technique described in Figure 9.c) uses resistive shunt and series feedback to set the input and output impedance. Amplifiers which use this technique usually have better high-power dissipation in comparison with other methods.

Last method shown in Figure 9.d) uses inductive source or emitter degeneration to create the resistive term in the input impedance. This process is more usual in GaAs amplifiers, but it has also been used in CMOS amplifiers at 900MHz as we can see in [22].

3.1.3 Design Configurations

The LNA design configuration is one of the most important parts of the receiver since it oversees providing enough amplification. Its design involves some important parameters which will provide different characteristics to the active device as noise figure, power gain, linearity, impedance matching, including DC power consumption.

In this report, we will present different design configurations whose characteristics are dedicated to different power applications well suited to high frequencies values nearly 5 GHz.

When designing an LNA, keeping attention on matching network is important in order to ensure efficient transfer and minimize power losses from the source to the load.

3.1.3.1 Common-gate (CG) topology

The common gate amplifier topology along with the common source amplifier topology are one of the most used amplifier topologies in radio frequencies (RF). This topology has a low noise figure at low frequencies, but it increases with frequency. Implementing another topology connected with a CG stage constitutes a cascode (CS+CG) amplifier and it is a good option in order to get higher gain, better noise performance, lower power consumption and higher isolation [23].

A common gate CMOS LNA is shown in Figure 10.

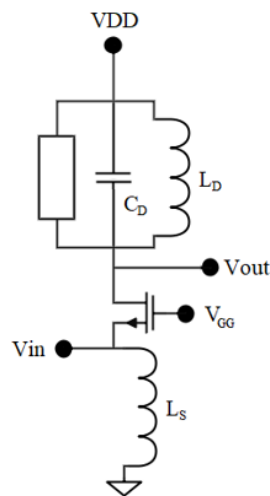


Figure 10. Common gate CMOS LNA [24].

If a stable circuit supplied by a low voltage is needed, CG configuration could be a good option, but this topology has a weak noise performance at high frequencies [18], [25], [26]. There are some techniques which can improve its characteristics as a capacitive cross coupling. With this technique, noise performance becomes better [27], [28], [29].

The voltage gain is given by the next equation

$$A_v = g_m \cdot Z_{out} \quad (2)$$

where g_m is the transconductance and Z_{out} is the output impedance.

Paying attention to Figure 10, we can see the output impedance is featured by the shunt LC tank. We know transconductance is almost constant while varying frequency, but the tank impedance is higher at its resonant frequency. Thus, we can ensure maximum LNA gain will be reached at the tank resonant frequency [16]. In

general, the inductor of the tank has worse quality than the capacitor, so the tank impedance is mostly limited by the inductor's quality. The tank impedance at the resonant frequency is given by

$$Z_{out} = Q_{LO}w_oL_o \quad (3)$$

where Q_{LO} is the quality factor of the inductor, w_o is the resonant angular frequency and L_o is the inductance of the tank inductor [6].

CMOS RF receivers usually need a common gate (CG) stage because it is easy to make the impedance matching and also has lower noise than other topologies [30].

One example of a CG LNA is the design created by David J. Allstot et. al [31]. They designed a common-gate LNA using a general g_m boosted technique using cross-coupled capacitors. They concluded that a g_m boosted CG LNA can provide better noise performance, and power consumption is lower than a conventional common gate (CG) or common source (CS) LNA. At a frequency of 5.6 GHz, CS and CG LNA exhibit a noise figure of 2.87 dB and 2.95 dB, respectively, while the g_m boosted CG LNA presents 1.69 dB of NF.

3.1.3.2 Common-source (CS) topology

Common source amplifier is one of the most used amplifiers in industry in CMOS analog circuits because it exhibits some advantages over common-gate (CG) LNAs such as lower NF or higher gain [32], [33], [34], [35]. Other characteristics of this topology are high input impedance, speed or simplicity. Basic CS LNA circuits are extensively used in CMOS RF integrated circuits because its stage provides superior noise figure performance. However, temperature, sensitivity to bias and component tolerances could be critical characteristics while trying to achieve best noise figure performance [17], [31].

In this topology the input signal is introduced into the gate terminal and exits the drain, and the only remaining terminal source is grounded. Typically, the output of a common source circuit is connected either a common drain (CD) stage or to a common gate (CG) stage in order to get better output results and better frequency characteristics [36]. The mixed configuration formed by a common-source (CS) stage and a common-gate (CG) stage is called a cascode amplifier. Cascode amplifier will be discussed in Section 3.1.3.3.

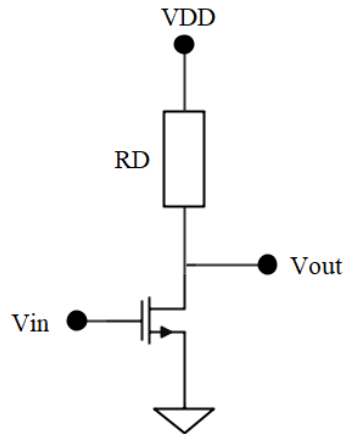


Figure 11. NMOS common-source amplifier.

One of the challenges when designing an LNA circuit is to create a 50Ω resistive input impedance. Best performance of the LNA is achieved if the input impedance is in the range between 25Ω and 100Ω . There is an important difference between the input matching network of a CS LNA and a CG LNA. The input matching in CS LNA is series resonant whereas in CG LNA is parallel resonant, which has a lower quality factor (Q). These characteristics of CG LNA make the parallel resonant network stronger against voltage or temperature variations [31]. C. Andriesei et. al [32] proposed a solution for matching the input of a CS LNA to the output of the last RF building block. In Figure 12, they illustrated a standard solution to get the goal. This solution consists in adding two inductors L_g and L_s to transform the capacitive input impedance into a resistance impedance, ideally 50Ω .

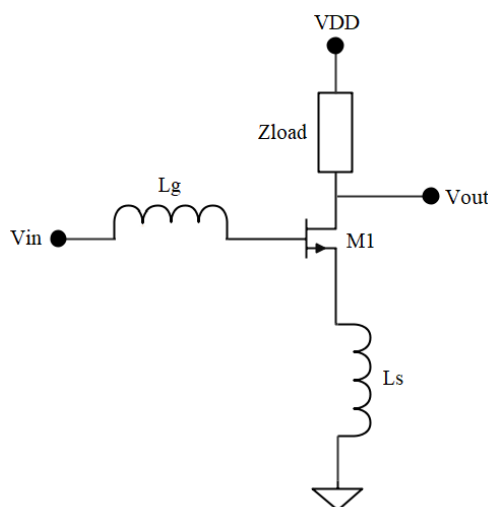


Figure 12. Common-source CMOS LNA with input matching [32].

A better topology based on common source for multi-band LNA design is the inductive degeneration common source topology (IDCS). IDCS consists in placing an inductor L_g in the source of a CS stage, as Andriesei et. al did. This inductor is used for creating a purely resistive input [37] which is noiseless, unlike other topologies in which a resistor is used to obtain the 50Ω impedance [31]. The source degeneration inductor provides a resistive input impedance because, ideally, the CS amplifier has only capacitance input impedance [37]. IDCS topology provides great noise performance but its bandwidth is narrow. A common source LNA with an inductive degeneration is shown in Figure 13 [38].

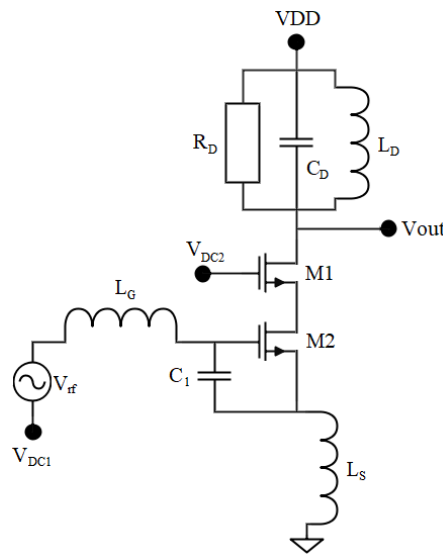


Figure 13. CS LNA with an inductive degeneration [38].

As we know, the main goal is getting maximum power gain, and to get this, it is necessary to have a resistive term. In common source topology, the input impedance is purely capacitive in low frequencies so a resistive part should be directly connected to the input impedance. This is done by a parallel resistive term in the gate or a degenerating inductance in the source of the CS transistor, as we can see in Figure 9 [18], [25]. In addition, this inductor makes optimum noise and power points to be close to each other [39]. The parasitic resistance of L_g consists of two parts. One is the spiral inductor whose quality factor is Q_{ind} , and parasitic series resistance, $R_{g,ind}$, and the other is the bond-wire inductor, L_{bw} , whose quality factor is Q_{bw} , and parasitic series resistance, $R_{g,bw}$. When Q_{ind} decreases, the quality factor of the input network also decreases. This results in a device that draws a large current which is the reason why capacitor C_1 is located between gate and source of the transistor. Now, the quality factor of the input network and the power consumption are not linked. In this way, the amount of power dissipated in the transistor can be controlled resulting in a power constrained design. [40]

The advantages of the IDCS topology, combined with the use of a multi-section input network, makes that a lot of narrowband systems work with this topology. Its good input noise properties can be used in wideband CMOS LNA designs [41].

An example of an IDCS CMOS LNA design is proposed by F. Ganesello et. al [42] who designed a 5 GHz LNA using 130 nm SOI CMOS technology for WLAN applications. Their design presents 1.4 dB noise figure and a gain of 14 dB at 5 GHz with a DC power consumption of 10 mW.

3.1.3.3 Cascode

The cascode topology is a multistage configuration. Is one of the most used topologies for radio frequency LNA in CMOS technology [20]. This topology mainly consists in a combination of two different topologies (CS+CG) connected one after another in order to get better characteristics as higher input and output impedance, higher bandwidth or better isolation between input and output. The cascode amplifier is a more versatile topology than common source and common gate topologies because it can achieve the widest bandwidth with a stable signal gain [17]. Having a higher bandwidth means there is a decrease in Miller effect which we will discuss in the next section.

Typically, a cascode amplifier as shown in Figure 14 is constituted from a first common source (CS) stage and another as a common gate (CG) stage. This combination provides an increase in the voltage gain and in the output impedance.

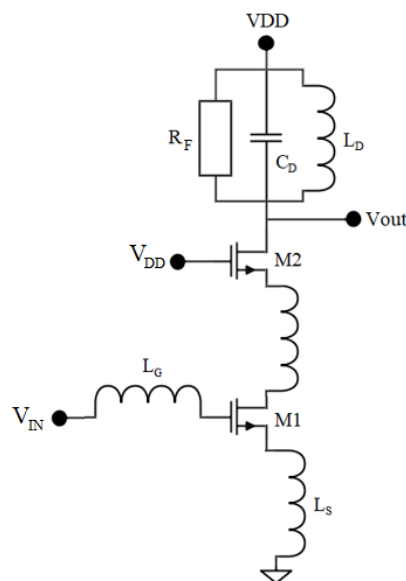


Figure 14. Cascode topology with source degeneration [24].

The first stage of the circuit is a common source amplifier in which the input signal is introduced into the gate terminal of M_1 . The following stage is a common gate amplifier which is the output of the circuit. As we can see in the Figure 14, the output voltage is taken from the drain gate of M_2 .

At high frequencies, we should take care about the different capacitances the transistors present. Otherwise, an imprecisely frequency response will be obtained. Cascode topology with source degeneration is widely used in LNA circuits with CMOS technology [23]. As we can see in Figure 14 there are two inductors L_s and L_g . The first of them, L_s is connected to the source of first transistor M_1 and it is the source degeneration inductor. The second one, L_g , connected at the gate terminal of same transistor M_1 is used for input matching [23].

An example of a cascode circuit design is the one made by S. Ambulker et. al [43] where they used a single stage common source amplifier followed by a common gate stage. Their design presents a gain of 14.4 dB and 2.04 dB of noise figure.

Some other authors have been studying different techniques for improving cascode topologies like T.S. Kim et. al [44] who applied the IMD Sinking Method to a cascode topology to improve linearity of the cascode LNA at the expense of lower gain and noise figure. The design with this technique implemented achieved an IIP3 of 13.3 dB which is an 8 dB improvement.

Miller Effect

Miller effect is the multiplication of the input capacitance times the voltage gain (Equation 4). This capacitance tends to reduce the bandwidth and, will be worse if it is increased because of the multiplication of the voltage gain. If bandwidth is reduced, the operation range will also be reduced, and the device could work improperly at certain frequencies. In Figure 16 it is shown how the equivalent circuit of an amplifier is considering Miller Effect.

At high frequencies, input impedance is almost zero because, as we know, the higher the frequency, the lower the impedance of a capacitor. If the input impedance is close to zero, then it can be considered as a short circuit and could cause serious damage to the circuit.

$$C_{Miller} = C(1 - A_V) \quad (4)$$

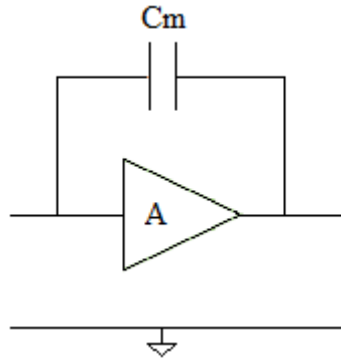


Figure 15. Amplifier with capacitance between input and output.

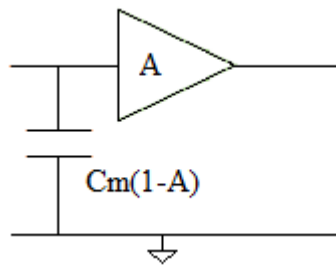


Figure 16. Effective capacitance circuit.

This effect can be reduced in different ways, by adding a voltage buffer stage in the input, by adding a current buffer stage in the output or with cascade topology [11].

3.1.3.4 Distributed amplifier (DA) topology

The distributed amplifier (DA) topology is made by two transmission lines connecting drain and gate pins of several active devices as shown in Figure 17. When the first active device input receives a signal, it propagates through the rest of devices one by one. All active devices respond to this signal and induce an amplification on the signal resulting the output signal in the output line. Each device adds a delay on the input signal which is caused by the lengths of the transmission lines and propagation constants [45].

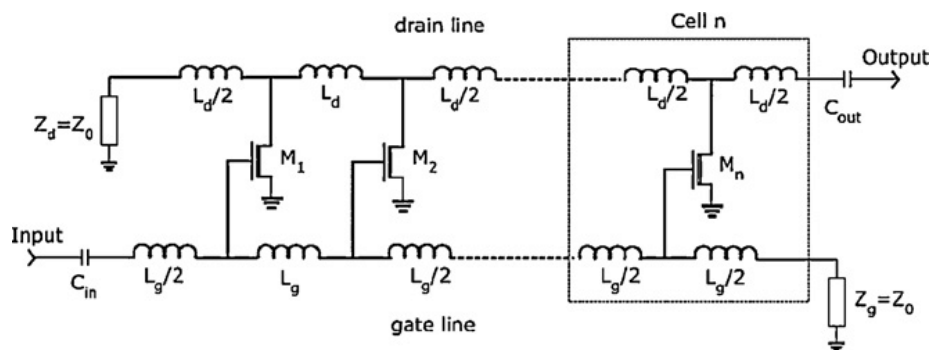


Figure 17. Distributed amplifier [46].

As we can see in Figure 17, each cell is separated using inductors which accumulate the gain of each transistor without any negative effects on the bandwidth. Main advantage of DA topology is that it has good input and output impedance matching but the high-power consumption they need to work properly, and the big size they occupy have both limited its applications [47]. A disadvantage of the CMOS distributed amplifiers (DAs) is that they present a high noise figure due to the thermal noise generated by resistive parts, especially the terminating gate resistor [48]. This, along the high-power consumption, made this architecture unattractive for LNA designers. However, authors like C. Aitchison [49] have demonstrated that the reverse gain of the distributed amplifier topology shields the noise generated by the terminating gate resistor located at the output, so noise figure is not limited by a 3 dB floor except at very low or high frequencies [47].

3.1.3.5 Differential topology

A differential amplifier is an active device that can increase the difference between two voltage inputs. There are two inputs and only one output which will be ideally the difference between the two inputs multiplied by a gain (A_d).

Differential topology is commonly used for CMOS LNA designs because it has some positive characteristics such as the possibility to connect its output directly to the differential input of the next active device block like e.g. a mixer [20].

This topology is characterized by two transistors which share the same drain terminal and will receive a bias current. The input of the circuit will be the gate terminal while the output will be the drain terminal of both transistors.

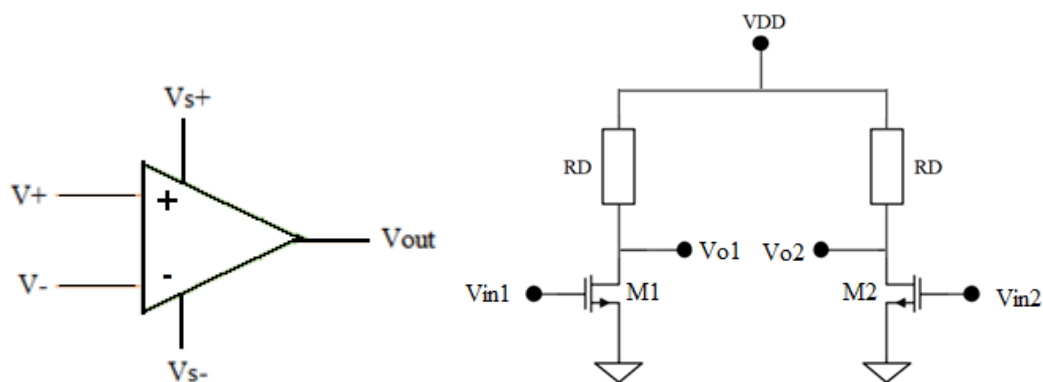


Figure 18. Conventional differential amplifier.

The output voltage of a differential amplifier is given by

$$V_{out} = A_d(V_{in1} - V_{in2}) \quad (5)$$

where $V_{in1} - V_{in2}$ are the input voltages.

Reality is different, thus if both inputs have same voltage, output voltage should be zero, but we notice this fact does not happen. Hence, we must consider this factor and add it to the equation.

$$V_{out} = A_d(V_{in1} - V_{in2}) + A_c\left(\frac{V_{in1} + V_{in2}}{2}\right) \quad (6)$$

where A_c is the gain when both input voltages are the same, called the *common-mode gain*.

A differential LNA provides good input matching and low noise figure. On the other hand, it is probably the power gain will not be enough to eliminate the undesired noise of the circuit. A differential capacitive cross coupled low-noise amplifier is shown in Figure 19.

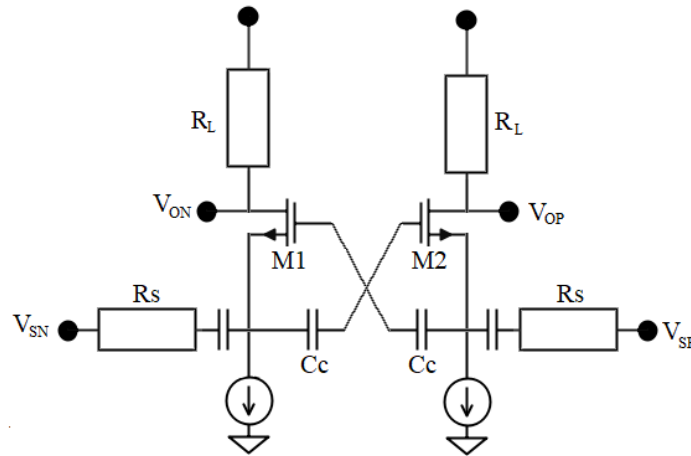


Figure 19. Differential capacitive cross coupled low-noise amplifier configuration [45].

The differential LNA is a better option over other topologies because external noise does not affect too much to the circuit, so linearity improves, and lower power is needed to feed the circuit in its input. The reason is that amplification of the signals attenuates the common mode signal, which is normally presented as noise in most systems [45]. Several authors have been designing different LNA with differential topology like Y.W. Hsiao et. al [50], Liao et. al [51] or F. Gatta et. al [52] among others.

3.1.3.6 Current reuse topology

The current reuse technique is used for reducing the power consumption of the amplifier maintaining high gain and low noise figure which make this technique very attractive in the ultrawideband (UWB) LNAs. This topology can be applied with any circuit configuration like cascode, CS or CG to reduce the DC power consumption of the LNA. The resistive current reuse amplifier, as shown in Figure 20, increases the transconductance of circuits and uses the reuse of DC current to save energy consumption. This technique is connected to a second stage, usually a common-gate stage acting like a buffer to improve the output impedance matching [45, 53].

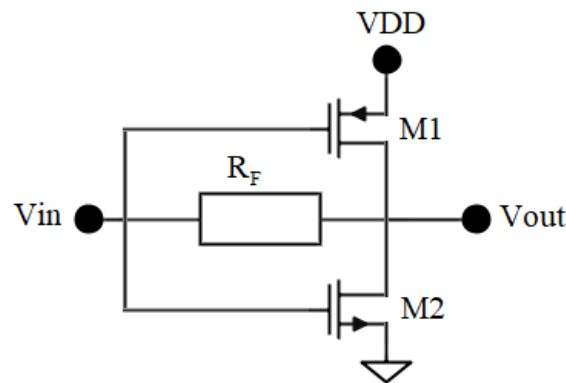


Figure 20. Resistive current reuse amplifier [53].

As we have said, this topology is used in conjunction with other circuits. In the case of J.S. Walling et. Al [54], they applied this technique to a CG-CS LNA to improve the gain performance. They also applied other methods like g_m boosting technique to improve noise performance. Other example of an LNA circuit implementing the current reuse technique is the one designed by T. Taris et. al [55] where they applied this method based on a one stage resistive feedback amplifier.

3.1.4 LNA Applications for 5 GHz

Over time, many designers have tried to improve characteristics of LNAs and used different topologies to reach the aim. In addition to attempting to improve LNA's key parameters, some authors have paid attention to the protection against electrostatic discharge. Electrostatic discharge (ESD) is an electrostatic phenomenon which causes an electric current flowing suddenly between two electrically charged objects. ESD has been one of the most critical issues in the IC industry. With the progress of nanotechnology, ESD is becoming worse due to the thinner gate oxide of MOS transistors [50]. Several authors have been working in this field as per Y. Hsiao et al [56] who designed a 5GHz differential LNA with pin-to-pin ESD protection using 130 nm CMOS technology which exhibits a power gain of 17.9 dB and NF of 2.43 dB at 5 GHz. Other authors like J. Borremans et al [57] also designed LNAs

with ESD protection. In this case, they achieved an LNA with a NF of 2.6 dB and power gain of 14.8 dB. Both LNA designs used a differential topology with 130 nm CMOS process. A deeper comparison with more LNA designs is shown in Table 1 and Table 2.

CMOS technology is commonly used in LNAs for wireless communications at gigahertz frequencies due to its low cost, high-level integration and high performance in terms of cutoff frequency [58]. Wireless local area networks (WLANs) working in 5 GHz frequency are being used for multimedia applications. Depending on the WLAN, it is necessary to design a transceiver which is suitable for each WLAN. In a receiver, the LNA must provide enough voltage gain and input matching with a low NF [59]. For applications above 5 GHz, CMOS technology presents low transconductance and signal loss through the conducting silicon substrate [42].

CMOS LNAs also have important functions in ultrawideband (UWB) systems. The Federal Communications Commission (FCC) authorized the UWB technology to be used in the frequency band between 3.1 GHz and 10.6 GHz. This technology can manage high data rate communications in short range applications. UWB was defined by the International Telecommunication Union (ITU) in 2006 as a “*technology for short-range radiocommunication, involving the intentional generation and transmission of radio-frequency energy that spreads over a very large frequency range, which may overlap several frequency bands allocated to radiocommunication services. Devices using UWB technology typically have intentional radiation from the antenna with either a –10 dB bandwidth of at least 500 MHz or a –10 dB fractional bandwidth greater than 0.2*”. Authors have been studying different techniques and configurations to obtain better performances in the design of the UWB LNA. Some examples of these designs are shown in Table 1 and Table 2, like M. Khurram et al [60] whose design exhibits a small signal gain (S_{21}) of 13 dB and a noise figure (NF) of 3.5-4.5 dB.

A standard FoM has been used in literatures to make comparisons between different LNA designs. Several authors [61], [62], [63], [64] defined the FoM of an LNA as

$$FoM = \frac{G \cdot IIP3 \cdot BW}{P_{DC}(NF - 1)} \quad (7)$$

where G is the small signal gain ($|S_{21}|$), IIP3 is the value of the third order input intercept point, BW is the bandwidth in GHz, PDC is the DC power consumption and NF is the noise figure in dB. There are some cases in which IIP3 can be substituted by P1dB. However, other ways for comparing different LNA designs are implemented.

Reference	CMOS Technology (nm)	Architecture	Gain ($ S_{21} $) (dB)	Frequency (GHz)	NF (dB)	S11 (dB)	P1dB (dBm)	IIP3 (dBm)	PDC (mW)
[42]	130	IDCS	14	5	1.4	-12	-*	-*	10
[50]	130	Differential w/ ESD protection	18	5	2.62	<-25	-*	-*	10.3
[50]	130	Differential w/o ESD protection	16.2	5	2	<-25	-*	-*	10.3
[57]	130	IDCS with ESD protection	14.8	5.5	2.6	-*	-*	-9	6.6
[60]	130	CS	13	3.1-4.8	3.5	-8	-15.4	6.1	-*

*Missing information.

Table 1. 5GHz LNA comparison with 130 nm CMOS technology.

Reference	CMOS Technology (nm)	Architecture	Gain (S ₂₁) (dB)	Frequency (GHz)	NF (dB)	S ₁₁ (dB)	P _{1dB} (dBm)	IIP ₃ (dBm)	PDC (mW)
[20]	180	Differential Transformer	14.2	5.75	0.9	-*	-*	0.9	16
[20]	180	Differential Cascode	14.1	5.75	1.8	-*	-*	4.2	21.6
[31]	180	CG	9	5.6	2.95	-39.6	-*	3.64	-*
[31]	180	CG + gm boosted	10.4	5.6	1.69	-16.4	-*	2.96	-*
[31]	180	CS	16.2	5.6	2.87	-28.1	-*	-5.1	-*
[37]	180	IDCS with ESD protection	20	5	3.5	-*	~20	-9	15
[43]	180	Cascode	39.788	5	2.045	-18	-*	-*	8.42
[51]	180	Differential + Current Reuse	12.5	5.7	3.7	-*	-11	-0.45	14.4
[54]	180	CG + Current Reuse + gm boosted	>20	5.4	<3	-*	-*	-*	2.7
[65]	250	Differential CS	16	5.25	2.5	-*	-*	-11.3	48
[66]	90	Cascode	14.5	3-5	2.2	<-10	-*	-*	8.2
[67]	90	Current reuse+Source follower	25	5	1	<-10	-*	-*	5 (nW)
[68]	90	Cascode + Source follower	25	0.5-8.2	1.9-2.6	-*	-*	-*	42
[69]	180	Inductively degenerated cascode	13.8	5	1.15	-12.4	-7	3	19.5
[70]	180	Inductively degenerated cascode	11	5	0.95	-33	-7	5	12

*Missing information.

Table 2. 5GHz LNA comparison with 90, 180 and 250 nm CMOS technology.

3.2 Up and Down Conversion Mixer

3.2.1 Background

A mixer is a nonlinear electrical circuit that is used to get new output signal frequency from two signals which are introduced in the input. The first input signal applied into the device is a radio frequency (RF) signal voltage and the other is a local oscillator (LO) voltage signal. These two frequencies are mixed in this nonlinear device and another two frequencies are obtained as a result. One of them is the sum of the input frequencies, and the other is the difference between them [71]. These frequencies are called “heterodynes”. In most applications, designers only need one of the heterodynes frequencies so the undesired one would be filtered out.

There are different classes of mixers. On the one hand, the most used ones are the commutating mixers. These use switches to change periodically the sign of the input signal which is controlled by a local oscillator. On the other hand, there are the non-linear mixers which employ cross-modulation to obtain the mixture of the input signals [72].

There are several electrical systems in which RF mixers are important for converting one frequency to another or changing in the signal phase.

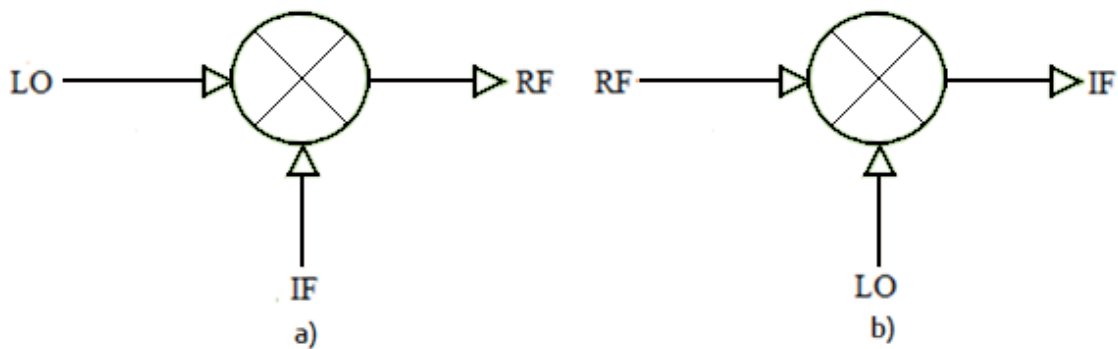


Figure 21. Frequency mixer symbol a) Up-conversion b) Down-conversion.

If we multiply two sinusoidal signals with different frequencies, the output result will contain a sum of the initial frequencies and a difference between them, as we can see in the Equation 8.

$$\cos(w_1t) \cdot \cos(w_2t) = \frac{1}{2} \cos(w_1t - w_2t) + \frac{1}{2} \cos(w_1t + w_2t) \quad (8)$$

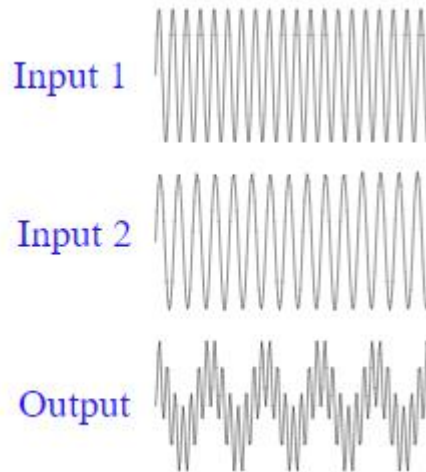


Figure 22. Two input signals mixed and the output as the result.

As an example of Figure 22, input 1 and input 2 are introduced into a mixer. As an output result, we can see a combination of these frequencies given by Equation 8. In many cases, designers usually add a filter to get only one of the frequencies obtained at the output. Depending on the system, the sum or the difference between both inputs will be filtered. In receiver systems, the sum will be suppressed, and the lower frequency called intermediate frequency will pass to next active block. However, in transmitter systems, the higher frequency, i.e. the sum of both inputs, will be the RF signal [73].

3.2.2 Conversion gain and conversion loss

Conversion gain and conversion loss are two of the parameters that designers look to improve in a mixer. Conversion gain for active mixers is the ratio of the intermediate frequency output power to the RF input power. Conversely, conversion loss for passive mixers is obtained as the difference between the input RF power and the desired output IF power, so the lower conversion loss, the more reliable circuit is. The typical values of CL in a passive mixer are between 4.5 to 9 dB [74].

3.2.3 Design configurations

When designing a mixer, one of the parameters that designers have always been concerned about is IP3. The big challenge is to filter the third order product. The tolerance level that a mixer supports is measured by IP3. Getting higher IP3 is possible by increasing local oscillator power or by having a better design [75].

3.2.3.1 Double-balanced CMOS Mixer

A double-balanced CMOS mixer is shown in Figure 23 where we can see that this topology consists of a pair of differential voltage switches. The pins of these switches are managed by the LO signals. Two of the switches are controlled by the positive phase of the LO and the other two switches are controlled by the negative phase of the local oscillator which has 180° difference. The switches will connect the RF and IF terminals alternately at the frequency of the local oscillator [72].

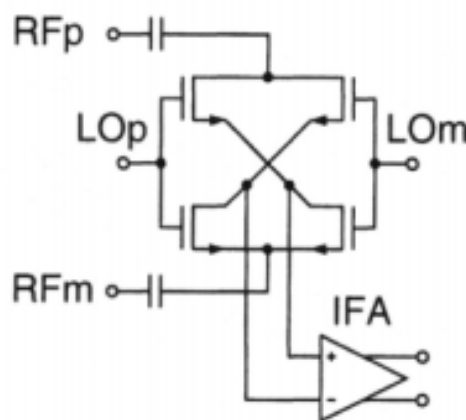


Figure 23. CMOS voltage mixer [72].

The noise figure of this mixer topology is mainly produced by the local oscillator driver. The mixer core consumes very low power, almost negligible, but the LO needs power to drive the input capacitance of the mixer. The size of the LO driver affects the noise figure, hence, we can say that the noise figure and the power consumption of the LO are related [72].

Double-balanced mixers can suffer distortion produced by device nonlinearities or phase modulation of the switchers. To improve the linearity, as per Walker et. al [76] the most important thing is to maintain a low current through the switches to reduce nonlinear voltage drops [72].

3.2.3.2 Gilbert Cell Mixer

Gilbert cell mixer is also popular in RF circuits. Unlike other types of mixers, the Gilbert mixer commutates the input signals in the current domain. The one in charge of converting the RF input voltage signal into a current signal is the M3 transistor that we can see in Figure 24 [6].

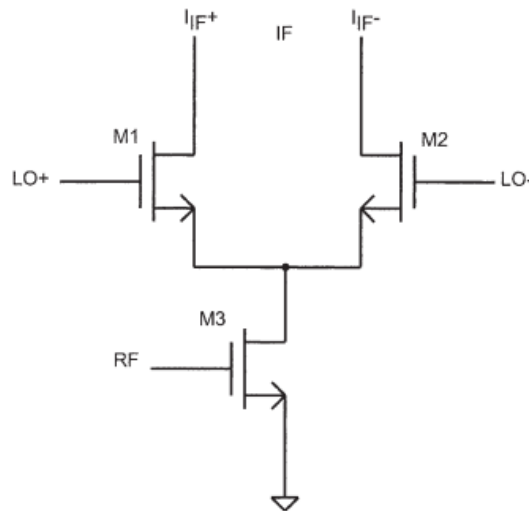


Figure 24. Gilbert cell mixer topology [6].

This topology provides good isolation between the local oscillator signal and the RF signal because there is not a direct connection from LO to RF. Nevertheless, due to the parasitic capacitances that exist between the gate and drain ports of the switches, the performance of the device can be adversely affected. This problem can be solved by using the double-balanced Gilbert mixer shown in Figure 25. The double-balanced Gilbert mixer can fix this drawback by using the couple differential technique. Double-balanced Gilbert mixer can remove the undesired LO and RF output signals from the intermediate frequency [6], [77].

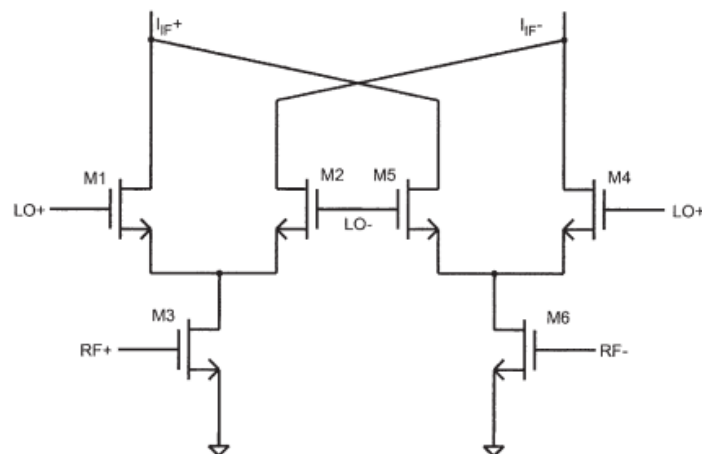


Figure 25. Double-balanced Gilbert cell mixer [6].

Designers usually modify the basic structure of the Gilbert cell mixer to achieve better results. A. Kara-Omar et. al [78] presented an example of up-conversion mixer using a new topology of mixer based on the Gilbert cell architecture. It was created to improve the input impedance matching over a bigger frequency range. Another technique used for improving the linearity of the Gilbert topology is described by W.-S. Hxiao et. al [79] who designed a Gilbert mixer with a current-reuse technique. Some other 5 GHz mixer designs are shown in Table 3 and Table 4.

3.2.4 Applications

Mixer converters are commonly used in radio transmitters, modems, satellite communications, radar, telemetry systems and phones, among others. The local oscillator can be either a sinusoidal wave or a square wave. These are commonly used in receiver front-ends and transmitter systems. In these systems, double balanced topology is the most used because the sum of input frequencies is filtered and only the intermediate frequency (IF) is seen at the output. In the case of a receiver, a down-conversion mixer is required, so inputs are RF signal and LO signal. Thus, the intermediate frequency will be seen at the output. On the other hand, in the case of transmitter systems, the IF signal is the input of the mixer and will be multiplied by LO to produce the RF signal [73]. Other configurations like Gilbert cells are also quite common in industry for implementing circuits, not only as frequency mixers, but also as variable gain amplifier, balanced modulator, phase detector or four quadrant analog multiplier.

With a mixer it is also possible to compare the phase of the input signals. The mixer will extract the phase difference between them and will be seen at the output [71].

In the medical field, the Wireless Body Area Networks (WBANs) are beginning to grow. WBANs are wireless communication network used by low-power devices placed in the human body. These networks are made up of electronic devices, such as sensors or microphones, with the aim of obtaining information on the vital signs of the patient. These components need to transmit the captured information being powered by small batteries. In line with these needs, designers have been studying the way of creating RF circuits powered with less than 1 V. M. Rahman et. al [80] designed a low-power low-noise mixer using 65 nm CMOS technology which could be powered with 0.7 V at a frequency range of 2.3-2.5 GHz.

In order to compare the performance of different mixers designs, there are many ways to express the figure of merit of a mixer. One common FoM is defined in [81] given by

$$FoM(dB) = \frac{CG[dB] \cdot BW[GHz]}{P_{DC}[mW]} \quad (9)$$

Reference	CMOS Technology (nm)	Frequency (GHz)	NF (dB)	Conversion Gain (dB)	IIP3 (dBm)	Power consumption (mW)
[79]	180	3.0-5.0	12-13	6.5	-*	11
[82]	130	3.0-11.0	-*	1.1	-*	9.7
[83]	250	3.1-5.0	8.4	3.8	-7.6	1.9

*Missing information.

Table 3. Comparison table of reported 5 GHz low-voltage CMOS UP-conversion mixers.

Reference	CMOS Technology (nm)	Frequency (GHz)	NF (dB)	Conversion Gain (dB)	IIP3 (dBm)	Power consumption (mW)
[84]	130	5.0	8	7 (CL)	10	-*
[85]	130	6.0-8.5	6.20-7.60	8	-*	6.0
[86]	130	5.0	12.7	11	12.15	4.0
[87]	180	3.17-4.75	14.6-19.8	3-8.7	-10.7-13.5	8.4
[88]	180	5.25	24.5	8.3	0.03	4.95
[89]	180	0.5-7.5	15	5.7	-5.7	0.48
[90]	180	5.1	19	27	-3	5.4
[91]	180	5.2	14	3.2	-8	0.8
[92]	180	3-8.72	6.80-7.30	2.5-5	5.0	10.4
[93]	180	5.8	7.8	15.7	-20.56	17.25**
[94]	180	5.7	14.6	-4.5	-*	10.8

*Missing information. **Shows the DC Power consumption of LNA + Mixer

Table 4. Comparison table of reported 5 GHz low-voltage CMOS DOWN-conversion mixers.

3.3 Oscillator

3.3.1 Introduction and General Background

The electronic oscillator is a device which provides an oscillating and periodic electric signal without an input AC signal. An oscillator converts DC power input into an AC waveform. In transceivers, the function of the oscillator is to provide the local oscillator (LO) signal which is connected to one of the inputs of the mixer.

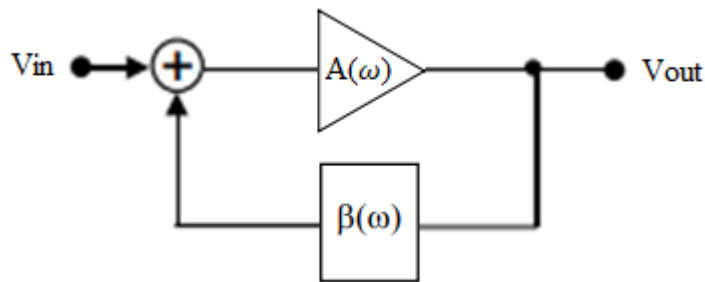


Figure 26. Block diagram with positive feedback [8].

Figure 26 illustrates a basic oscillator block diagram with feedback where A is the gain of the amplifier and β is the feedback transfer function. $(A \cdot \beta)$ is the gain of the global loop. Magnitude and phase of these terms vary with angular frequency, ω . The input and output signals must be in phase. Thus, the phase shift of the feedback must be either 0° or 360° . If phase shift is 180° , an inverted output is obtained. Gain of the loop is given by

$$A_V = \frac{V_{out}}{V_{in}} = \frac{A}{1 - (A \cdot \beta)} \quad (10)$$

The behaviour of the circuit can be predicted by knowing $|A\beta|$ and the phase of the gain loop, $\varphi_{A\beta}$:

- If $|A\beta| < 1$, the circuit is stable.
- If $|A\beta| = 1$ and $\varphi_{A\beta} = 0$, the output frequency will be the same as the input frequency maintaining the amplitude of the signal.
- If $|A\beta| > 1$ and $\varphi_{A\beta} = 0$, any frequency at the input will be amplified until the amplifier goes into saturation region.

These conditions are known as the *Barkhausen Criterion*. These need to be satisfied in order to obtain oscillations in a circuit. However, it is important to note that these conditions are necessary but not sufficient.

3.3.2 Ideal LC Tank

The most basic ideal oscillator is composed by two elements: a capacitor and an inductor as shown in Figure 27.

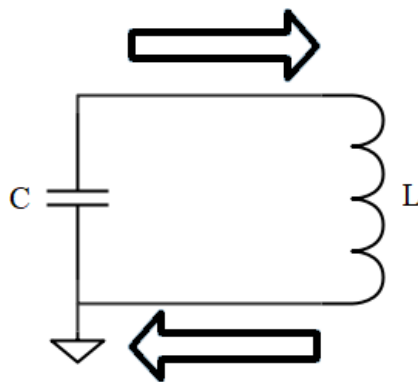


Figure 27. Most basic LC oscillator.

Let's assume the capacitor is initially charged. Current will flow from the charged capacitor to the inductor, so the capacitor is discharging, and the inductor is being charged. While the current flows through the inductor, a magnetic field is created, and it grows as the current increases. This will happen until the capacitor is totally discharged. At that moment, the current will decrease and thus the magnetic field produced by the inductor will also decrease. When the magnetic field collapses, the inductor releases the stored energy taken from the capacitor, so it is putting back that energy into the circuit. Another consequence due to the collapse of the magnetic field is that the polarity across the inductor will be reversed, so now, the inductor is releasing its energy and the capacitor is getting it and therefore being charged again. At this point, we can see that while one element is being charged, the other is being discharged. The current is always varying, forming an oscillation. Due to the circuit resistance, energy will be dissipated in the form of heat and the amplitude of the oscillation will be smaller and smaller. By applying some periodical energy to the circuit, the problem is solved, and the amplitude of the oscillation is maintained.

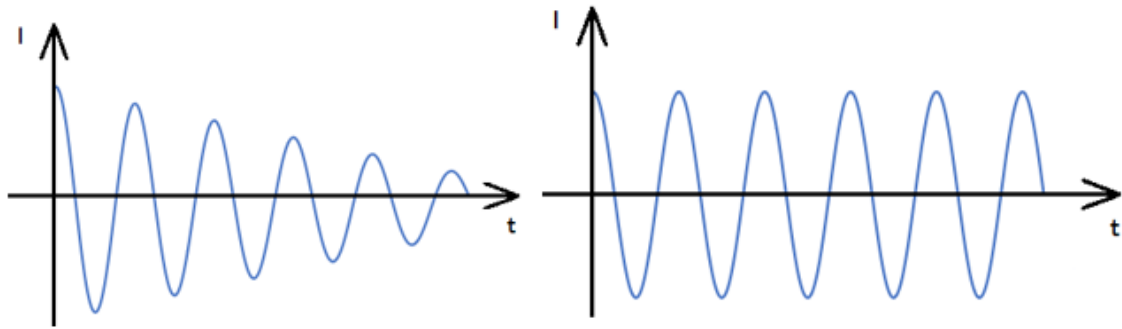


Figure 28. Oscillation of the basic LC oscillator a) with no feedback b) with feedback and energy supply.

3.3.2.1 LC Tank Properties

In practice, losses from inductor and capacitor must be taken into account. Figure 29 illustrates a LC tank modelled with a parallel and series resistor, respectively. Series resistance tank is preferred over the parallel resistance tank because it is closer to the physical losses in integrated inductor [95]. Figure 29.b) can be transformed in Figure 29.a) with

$$R_p = \frac{L_s}{R_s C} \quad (11)$$

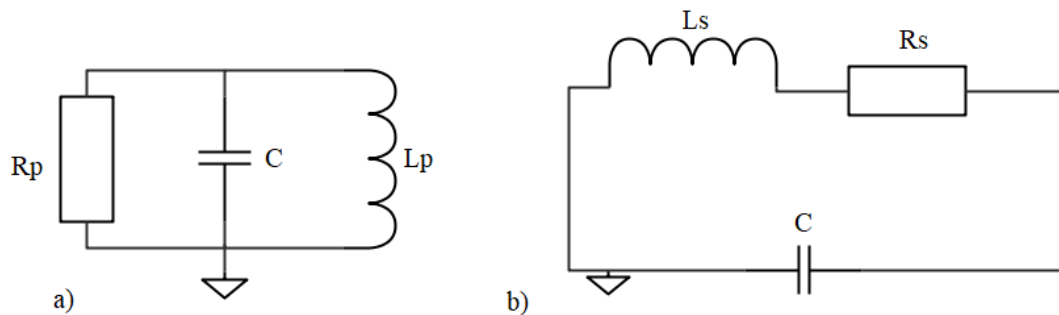


Figure 29. LC tank a) parallel b) series.

Depending on the values of the components, different output voltage cases are possible. Situations on a parallel LC tank are described and shown in Figure 30.

- 1) If $R > 0$ and $R^2 < L/4C$, stable case.
- 2) If $R > 0$ and $R^2 > L/4C$, as first situation, has a stable response. Both cases are commonly used in passive RLC circuits.
- 3) $R = \pm\infty$, refers to oscillations with constant amplitude.
- 4) $R < 0$ and $R^2 > L/4C$, its amplitude oscillation increases over time.
- 5) $R < 0$ and $R^2 < L/4C$, the output voltage does not oscillate. Situation number 4 and 5 belongs to unstable cases.

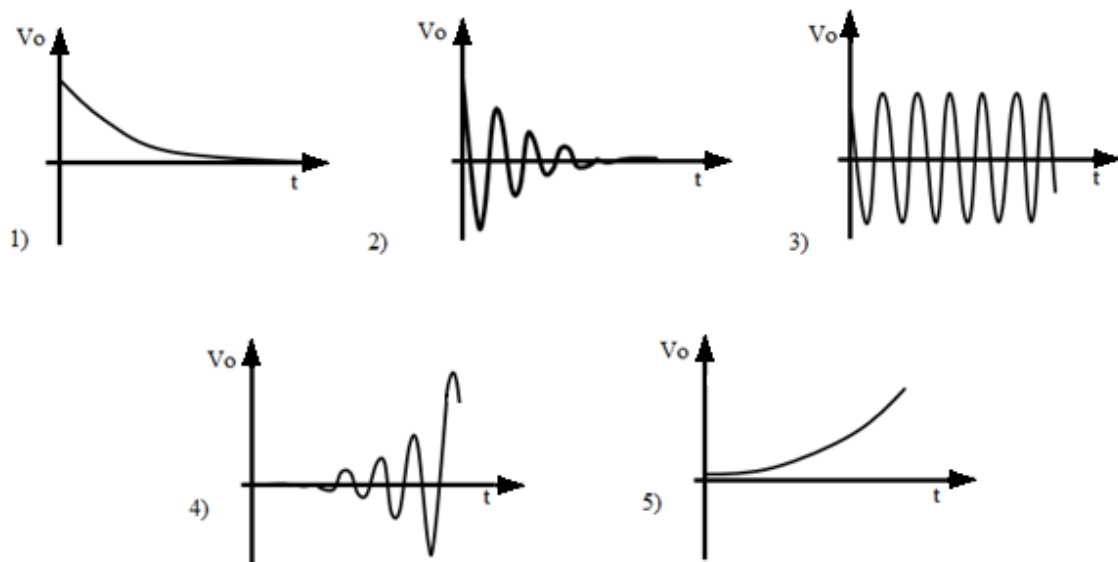


Figure 30. Possible parallel LC tank solutions.

3.3.3 Oscillator parameters

3.3.3.1 Negative Resistance (NR)

As situation 4 and 5 show in last section, LC circuits are linked to negative resistances. This resistance is necessary to compensate energy losses related to the parasitic resistances of the capacitor, and mainly, of the inductor. Initially, the total equivalent resistance must be negative in order to get oscillations with increasing amplitude. Then, the amplitude of the oscillator stabilizes, and the oscillation frequency is the resonant frequency of the circuit given by

$$\omega_{osc} = \frac{1}{\sqrt{LC}} \quad (12)$$

3.3.3.2 Phase Noise

The phase noise of an oscillator is the ratio of signal power to noise power measured in frequency domain. Phase noise is an important limitation in wireless communication channels due to possible interferences from undesired frequencies. Phase noise has become one of the biggest problems for designers over the years. It is an even more critical parameter for oscillators than output power since it can degrade the performance of communication and radar systems. In many applications, it is important to keep the phase noise as low as possible, even at the expense of the output power [5].

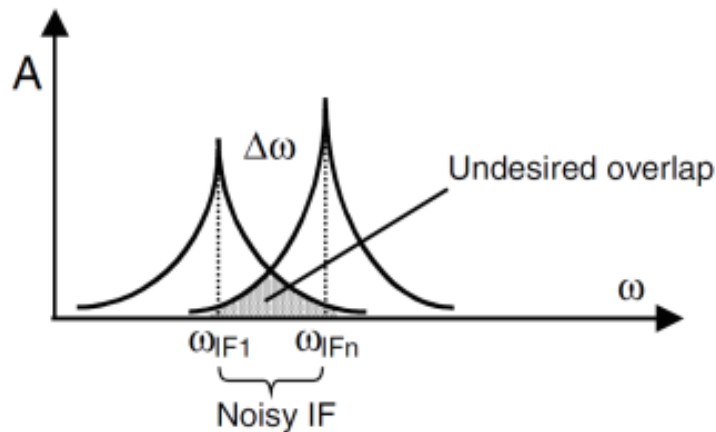


Figure 31. Possible interferences caused by phase noise [8].

Figure 32.a) illustrates the frequency spectrum of an ideal oscillator with zero phase noise. However, in practice, the signal produced by an oscillator is the mixture of multiple signals. The principal signal is known as *frequency carrier*, f_o . There are other signals occurring simultaneously around the carrier having frequencies $f_o \pm f_m$, where f_m is the offset frequency from the carrier frequency. An oscillator with high phase noise produces large undesired side-band noise signals which could produce degradation on the performance of the devices. The smaller the side-band signals, the better the performance of the device, which is possible with a very low phase noise oscillator [5].

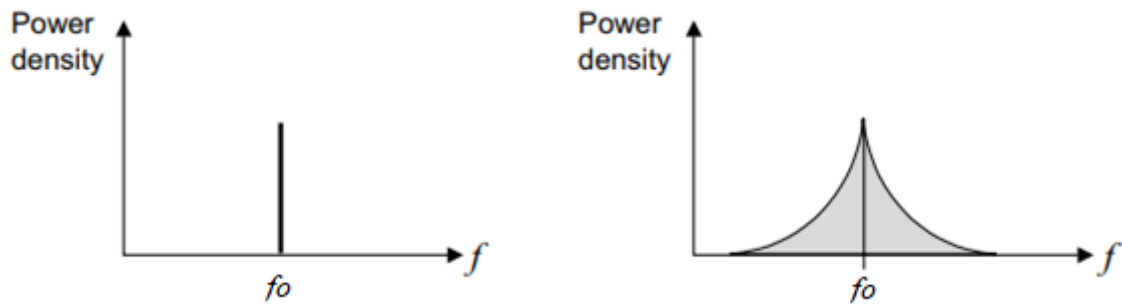


Figure 32. Frequency spectrum of a) ideal oscillator b) real oscillator [95].

Digital circuits are affected by physical noise by nature, but they also add additional noise in switching operations. The most common noise types are flicker, shot and thermal noise [96].

- *Flicker noise*, also known as *1/f noise*, manages the noise properties which appears at low frequencies, lower than 1 MHz. *1/f* is caused by random charging and discharging of impure spots in devices. Most of these impurities can be found in the surfaces of semiconductors. The longer a current flows along the surface, the higher the probability of trap charging is. That is the reason why flicker noise is inversely proportional to the frequency (*1/f*). The level of the flicker noise varies depending on the type and characteristics of the transistor used. BJTs usually present lower flicker noise than CMOS transistors, and consequently, CMOS oscillators have higher *1/f* phase noise [5].
- *Shot noise* is referred to noise generated when current flows through a potential barrier. Electrons can spend time in one or another terminal arbitrarily and it is when noise appear. The shot noise increases with DC current [8].
- *Thermal noise* is generated by every ohmic resistor. Thermal noise is directly related to frequency so that as the bandwidth increases, thermal noise also increases [8].

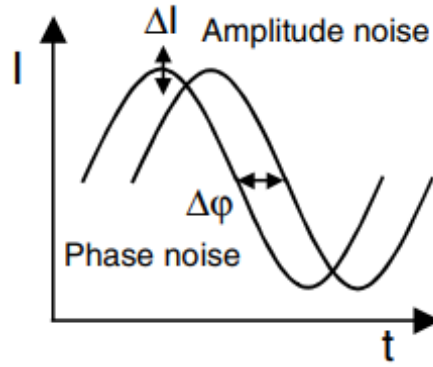


Figure 33. Amplitude and phase noise in time domain [8].

In time domain, the output current of an ideal oscillator would be given by

$$i(t) = I \cdot \cos(\omega_{LO} \cdot t + \varphi) \quad (13)$$

where I is the amplitude, ω_{LO} is the angular frequency and φ is the phase. In reality, Equation 13 changes and noise must be added as shown in Figure 33.

$$i(t) = (I + \Delta I) \cdot \cos(\omega_{LO} \cdot t + \Delta\varphi) \quad (14)$$

Normally, as the oscillators work in saturation, the amplitude is constant, and variations are almost eliminated. However, the phase of the signal can be affected, and it is more important when designing an oscillator. There are some strategies to minimise the phase noise like improving the local oscillator power or having a high quality resonator [8].

3.3.4 Voltage Controlled Oscillator (VCO)

A voltage-controlled oscillator (VCO) is an electronic device whose frequency can be controlled by an input voltage signal, called “Control Voltage (CV)”. When the VCO is connected to a suitable voltage supply, an oscillating output is seen in the output terminal. The output voltage is given by the next equation,

$$V_{out} = A \sin(\omega_c t + \phi) \quad (15)$$

where A is the amplitude, ϕ is the phase and ω_c is given by

$$\omega_c = 2\pi f_c \quad (16)$$

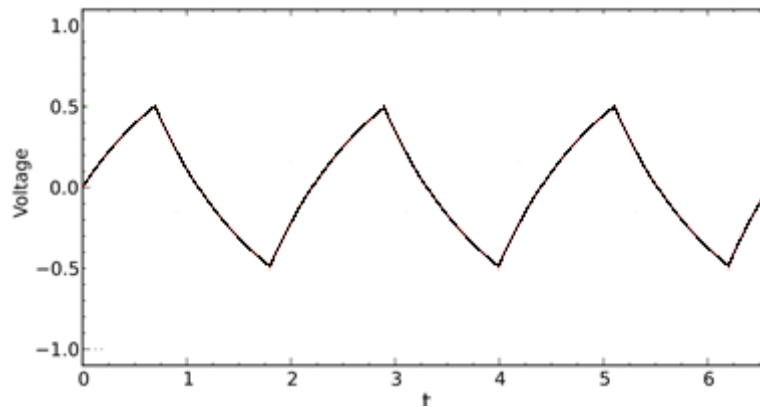


Figure 34. Triangular waveform from a relaxation oscillator.

VCOs can be classified into two main groups depending on the type of waveform produced: harmonic or relaxation oscillators.

- Linear or harmonic oscillators: the output signal produced is a sinusoidal waveform.
- Relaxation oscillators: the output signal produced is a triangular waveform. This oscillator needs a capacitor located in the output. The triangular waveform shown in Figure 34 is formed thanks to the charge and discharge of the capacitor.

3.3.4.1 Colpitts Oscillator

Figure 35 shows a single-ended Colpitts oscillator using CMOS process. The Colpitts oscillator uses two capacitors in series with a parallel inductor forming the resonant tank. Another capacitor could be used at the output of the circuit to filter out the DC component. The frequency of the output signal varies depending on the value of C_1 , C_2 and L_1 , and it is given by

$$f = \frac{1}{2\pi\sqrt{LC_T}} \quad (17)$$

where C_T is the capacitance of both series capacitors C_1 and C_2 .

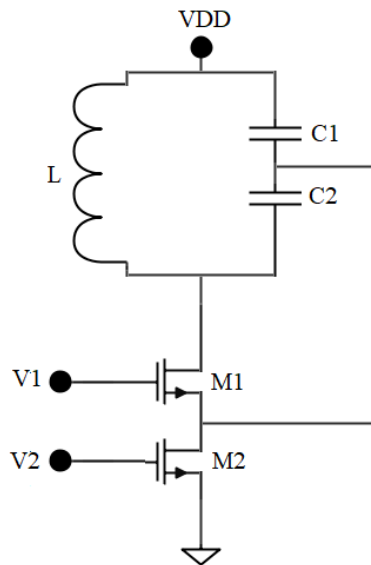


Figure 35. CMOS single ended Colpitts oscillator [97].

There are variations of Colpitts configuration in order to reduce the effects of the noise. Ilias Chlis et al [97] explained three different techniques for phase noise reduction using CMOS technology: inductive degeneration, noise filter and optimum current density.

3.3.4.2 Cross-Coupled Oscillator

Cross-coupled oscillator as shown in Figure 36 uses RLC as the element which determines the oscillation frequency. This topology is one of the most used VCO configurations when using CMOS technology. CMOS VCOs present higher input impedance than HBT VCOs, resulting in a better-quality factor of the LC tank. The quality of the resonator is mainly featured by the inductor, since capacitors have very high-quality factor and it is considered that they present insignificant losses [5].

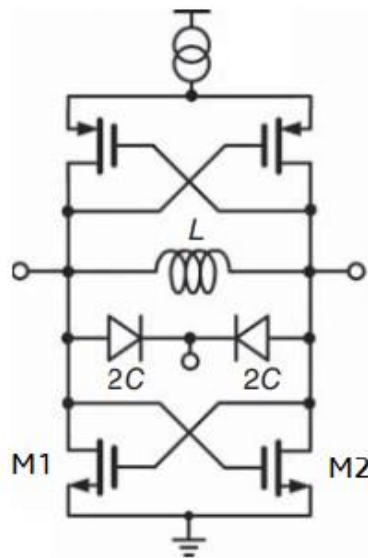


Figure 36. Cross-coupled VCO using CMOS [5].

In figure above, a cross-coupled VCO is illustrated using complementary NMOS and PMOS, but it is also possible to use only NMOS or only PMOS. As we discussed in Section 3.3.3.1, an oscillator must have a negative resistance to maintain an oscillation over time. To provide the necessary negative resistance, a positive feedback is obtained using the two cross-coupled transistors M1 and M2 [5].

3.3.4.3 Ring Oscillator

Ring oscillator circuit is configured with the connection of amplifiers in a ring. Ring connection means the output of the last block is fed back to the input of the first one. The ring will oscillate only if the phase shift over the ring is 360° [95]. This topology is configured by n stages which are coupled back. The number of cells which are connected in the loop is the main basis of ring oscillators. When designing the oscillator, it is important to consider the application in which it will be used in order to choose the number of cells. Two, three or four cells are common architectures in wireless communication system designs [98].

This kind of circuits are well integrated because of their small area, but the principal disadvantage is these need high power consumption to work properly and these also have high phase noise. CMOS technology is a good option in this oscillator because it presents good performance working with DC power [8].

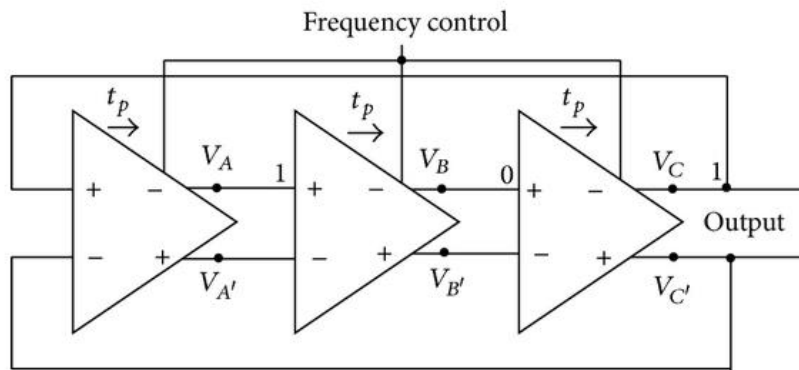


Figure 37. 3-stages ring-VCO [98].

The main advantage of ring oscillators is that these need only transistor and resistors. However, the frequency is limited because, as we said, ring oscillator needs at least three inverter stages, so maximum frequency will be determined by the parasitic of these three stages [8].

It is important to have, at least, three single inverter stages to get a periodic variation of the voltages. The implementation of four stages in the ring oscillator design consumes much more amount of power due to the additional stages. The 3-stages oscillator is faster than the 4-stages RO and, it also reduces the power consumption. Figure 37 illustrates a ring oscillator designed by J. Jalil et al [98] in which they only used three differential amplifiers.

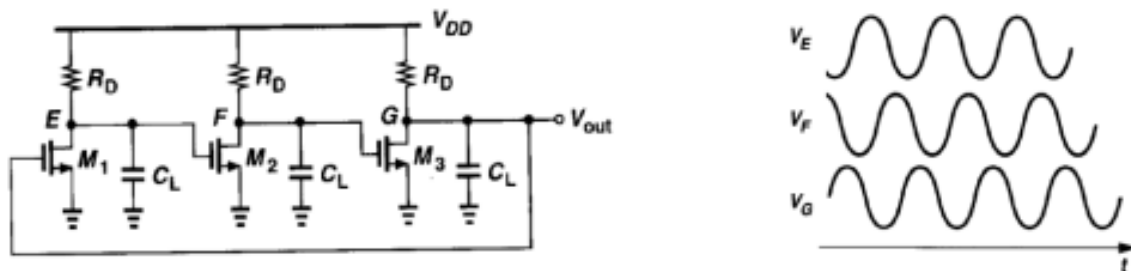


Figure 38. Three stages oscillator [3].

In [99], some authors have designed a ring oscillator with an oscillation frequency of 13GHz using nine stages with 90 nm SOI CMOS technology. If only three stages were used, the oscillation frequency could be increased up to 39 GHz.

3.3.4.4 Figure of Merit of a VCO

The voltage-controlled oscillator is an important device in RF signal processing. Its main aim is to minimize the phase noise and the power consumption [24]. As we said, the VCO is used for generating the LO signal connected to the mixer. The efficiency is given by the relation between LO output power and required DC power. Thus, one commonly used way of comparing VCOs is considering the output power generated by the device. The figure of merit is given by [24]

$$FOM_{VCO} = \left(\frac{f}{\Delta f} \right) \cdot \frac{P_{OUT}}{L[\Delta f] \cdot P_{consumption}} \quad (18)$$

where f is the oscillation frequency, Δf is the frequency offset, P_{OUT} is the power generated at the output, $L[\Delta f]$ is the phase noise evaluated at the frequency offset and $P_{consumption}$ is the power consumption.

FoM of an VCO must be evaluated at the frequency where maximum phase noise is achieved. Phase noise varies depending on parameters like the quality of the LC tank (which determines the oscillation frequency), the amplitude of this oscillation, and possible noise added, produced by active and passive components of the VCO. The amplitude of the oscillation is limited by the maximum permissible voltage of the transistor [24].

Another common way of comparing different VCOs is using the phase noise figure of merit. Noise performance of a voltage-controlled oscillator depends on the frequency offset. Thus, the higher the frequency offset, the lower the phase noise. This FoM [8] is given by

$$FoM = L(\Delta\omega) - 20 \log \left(\frac{\Delta\omega}{\omega_{LO}} \right) - 10 \log \left(\frac{[mW]}{P_{dc}[mW]} \right) \quad (19)$$

where $L(\Delta\omega)$ is a concept which measures noise floor, resonator noise and flicker noise explained by Ellinger [8].

Reference	Architecture	CMOS Technology (nm)	Centre Frequency (GHz)	Phase Noise (dBc/Hz)	Supply (V)	Tuning range (MHz)	Power DC (mW)
[100]	Class-C	130	4.9	-132.8	1	685	1.4
[101]	LC VCO	130	5.17	-122.3	0.4	2200	0.495
[102]	DM VCO	130	4.9	-117.6	1.2	1900	9
[103]	DM VCO	130	5.7	-104	1	4200	8
[104]	UWB VCO	130	5.6	-75.42	1.8	3600	29.1
[105]	LC VCO	130	5.225	-110	1.2	450	12
[106]	Differential Colpitts	130	4.9	-132.6	0.4	122.5	1.92

*Missing information.

Table 5. Comparison table of reported 130 nm CMOS VCOs.

Reference	Architecture	CMOS Technology (nm)	Centre Frequency (GHz)	Phase Noise (dBc/Hz)	Supply (V)	Tuning range (MHz)	Power DC (mW)
[5]	Cross-coupled	250	5.2	-117	1.8	1300	-*
[5]	Distributed	180	15	-100.2	1.8	1700	34.2
[98]	RO	180	1.5	-126.62	1.5	2000	2.47
[107]	LC VCO	180	2.5	-128.7	1.8	275	5.4
[108]	TF VCO	180	1.4	-129	0.35	0	1.46
[108]	TF VCO	180	3.8	-119	0.5	320	0.57
[109]	Multi-band VCO	180	5	-125	1	200	6
[109]	PMOS	180	5.21	-127	1	420	4.2
[110]	Cross-coupled	180	7.128	-111.2	1	330	2.2
[111]	Differential Colpitts	180	5.46	-100.3	1.8	580	6.4
[112]	LC VCO	250	1.3	-142	2	200	14
[113]	Cross-coupled quadrature	250	1.86	-143	2.5	280	20
[114]	Push-push	250	63	-85	1.8	2520	119

*Missing information.

Table 6. Comparison table of reported 90, 180 and 250 nm CMOS VCOs.

3.4 Power amplifier (PA)

3.4.1 Background

Power amplifiers are used in the last stage of a radio transmitter to amplify the power level before the signal is sent to the antenna. In the case of an audio receiver, the power amplifier delivers the necessary power so that the speaker can reproduce the received signal. This device plays an important role for the global efficiency in a transceiver system since it is the one that operates between the radio frequency system and the antenna. Nearly all power amplifiers are nonlinear and present a power limit to be amplified. The nonlinear behaviour of PAs can be measured by AM-to-AM or AM-to-PM responses explained later in Section 3.4.2.2. PAs have been an important research over the years to find ways to provide competitive power and area efficiency. CMOS technology applied into power amplifiers is a suitable solution to achieve lower costs, high-density and full integration, resulting in increasingly smaller chips [115, 116]. Power amplifiers can be divided in two main groups: linear or amplification-mode PAs and nonlinear or switch-mode PAs.

Linear amplifiers group involves such amplifiers which are intended to operate in its amplifying region. Main objective designers look for is the trade-off between linearity and efficiency. As we will see in next sections, the most linear power amplifiers are those in which the transistor is always conducting, as Class A PA [117].

Nonlinear PAs involve such amplifiers in which the transistor operates as a switch. For RF applications, the two most used classes are Class D and Class E which will be described in Section 3.4.4.1 and Section 3.4.4.2, respectively.

3.4.2 Basic PA Parameters and Characteristics

3.4.2.1 Drain and Power-Added Efficiency

As we said, power amplifiers are usually the most power consuming device in a transceiver system, thus, amplifier efficiency is an important parameter. The efficiency of an amplifier can be measured with the *drain efficiency* concept which is the ratio between RF output power and DC input power.

$$\eta_{DC} = \frac{P_{out}}{P_{DC}} \quad (20)$$

where P_{out} is the RF output power delivered to the load and P_{DC} is the DC power from the power supply. For ideal power conversion, the efficiency is 1. When a high amplification is needed, one single stage of amplification may not be sufficient. Some

PAs require more than one amplifier stage to achieve the desired power level while maintaining the stability of the overall system. In these cases, η_{DC} only represents the efficiency of the final stage [118].

Drain efficiency does not take into account the RF power delivered at the input of the amplifier. There is another way of measuring the efficiency called *power-added efficiency (PAE)* which considers the RF input power, P_{in} . PAE is a more widely used FoM than drain efficiency because it includes the amplifying RF input signal as well as the DC power consumption.

$$PAE = \frac{P_{out} - P_{in}}{P_{DC}} = \eta_{DC} \left(1 - \frac{1}{G}\right) \quad (21)$$

where G is the power gain. As we can see, if the power gain is high enough, it can be said that power-added efficiency is practically the same as the drain efficiency, η_{DC} .

3.4.2.2 Linearity

AM-to-AM and AM-to-PM

Linearity is a fundamental parameter in a power amplifier design. Good linearity means the amplitude and phase of the signal are preserved, so the signal can be transmitted successfully. For measuring the linearity there are some ways like AM-to-AM (amplitude modulation to amplitude modulation) or AM-to-PM (amplitude modulation to phase modulation) relations. AM-to-AM compares the amplitudes of both input and output signals. AM-to-PM compares the amplitude of the input signal with the phase of the output signal [118], so we can measure easily the undesired phase deviation caused by the amplitude variations at the input.

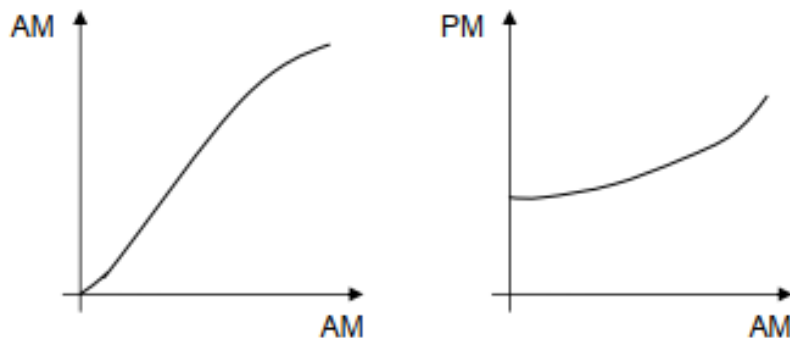


Figure 39. Graphics representing linearity of a PA: a) AM-to-AM b) AM-to-PM [118].

Linearity can be measured with another two general parameters: the output *spectral mask* and the *error vector magnitude (EVM)* of the output signal. The spectral mask concept deals with the protection of communication channels in the system due to added noise generated by transmission devices which are not using a frequency within the bandwidth [119]. The EVM is the length of the vector which connects the ideal I/Q signal vector to the I/Q measured signal vector. Noise and distortion can degrade the EVM which means the amplifier will present worse linearity [120].

Power amplifiers can be classified in different classes depending on their operation. The fundamental classes are A, B and C. Other configurations, such as classes D, E or F, have been developed from the first ones. These tend to have a higher efficiency than the fundamental classes. In both cases, a high-Q resonator tank is connected at the output to operate as a bandpass filter.

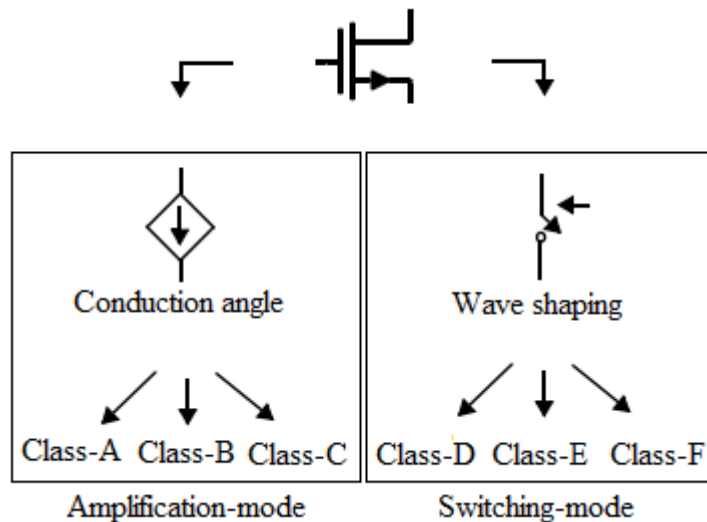


Figure 40. Power amplifiers divided by classes [121].

3.4.3 Amplification-mode PA

This group involves classes A, B and C. These present same collector voltage waveforms. The difference between these topologies lies in the angle of conduction and in the shape of the waveforms. Class AB also belongs to this group. It was the main option for designers for many years since it provides the linearity of Class A and the efficiency of Class B PAs [121]. Theoretically, linear amplifiers provide an identical output signal as the input but at a higher power level.

3.4.3.1 Class A

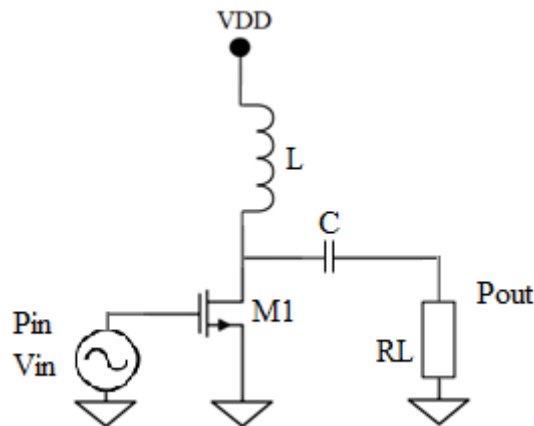


Figure 41. Single-stage Class A PA [122].

The main characteristic of Class A PA is that its transistor never turns off and it is always conducting. This topology operates as a linear power amplifier and the transistor functions in the active region [5]. There is a common concept used in power amplifiers called *conduction angle*. Conduction angle is defined as the part of the input signal during which the transistor conducts. In Class A, the transistor is always conducting, so it presents a conducting angle of 360° as shown in Figure 42.

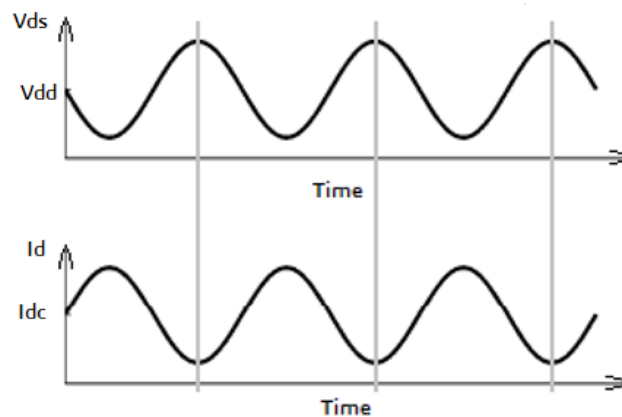


Figure 42. Drain voltage and current waveforms for Class A PA [119].

When an active device switches off, distortion can appear affecting the linearity of the power amplifier. Class A active devices never turn off, so nonlinearities are not introduced. Class A PAs are considered to be the most linear of all classes due to this reason, but its maximum efficiency is 50%, assuming linear transconductance. In practice, the efficiency of a Class A amplifier is less than 30%. An example of this class is the PA implemented in a 65 nm CMOS process designed by T. Quémerais et al [123]. Their amplifier presents a power gain of 13.4 dB and an output P1dB of 12.2 dBm with 7.6% PAE. It can be compared with other designs in Table 8.

3.4.3.2 Class B

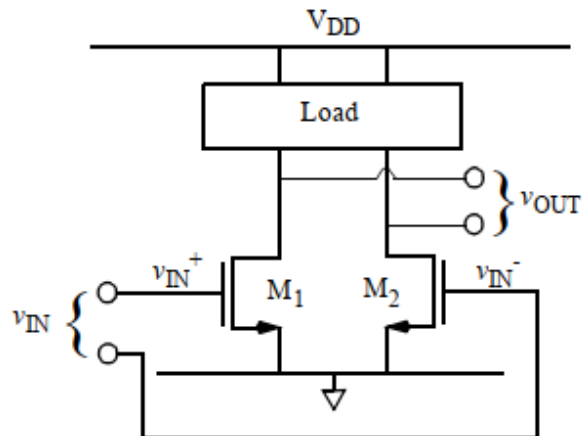


Figure 43. Differential Class B PA [117].

Class B PAs are quite similar to Class A PAs since they use same way of operating but are biased differently. In this case, the transistor only conducts half of the RF cycle, as it is shown in Figure 44. Hence, the conduction angle for a Class B PA is 180° .

Unlike Class A PAs, the active device used in a Class B PA is operating intermittently. As we said, when an active device turns off, some distortions can appear on the output voltage. Thus, it is necessary to have a better-quality tank in order to reduce this distortion. This class presents worse linearity than Class A amplifiers due to this reason. However, assuming linear transconductance, a Class B PA can reach 78.5% efficiency.

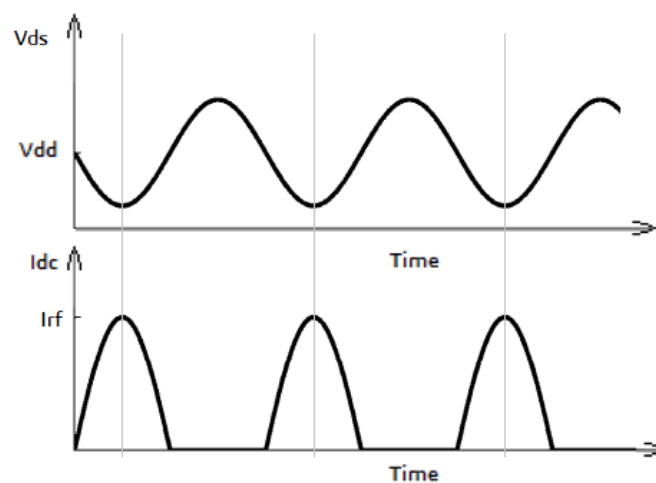


Figure 44. Drain voltage and current waveforms for Class B PA [119].

In Figure 45 is shown a Class B PA called *push-pull* formed by two complementary CMOS transistor connected at the same input. In this case, each transistor will conduct only one part of the sinusoidal signal received in the input. M1 will conduct the positive part of the signal, while M2 will conduct the negative part. Thus, both transistors will operate intermittently resulting a conducting angle of 180° . Transistors working at half period than in Class A will present less heat dissipation resulting better efficiency. However, when the input signal is not high enough to excite the transistors, distortion occurs. This distortion is called *crossover distortion* and it is illustrated in Figure 46. There are some authors who have been designing amplifiers trying to reduce the crossover distortion like A. Beohar et al [124].

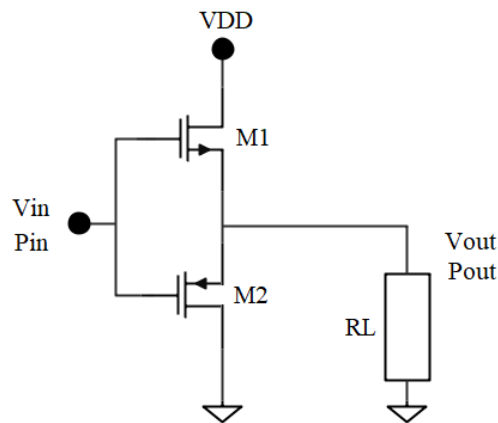


Figure 45. Pull-push CMOS Class-B PA.

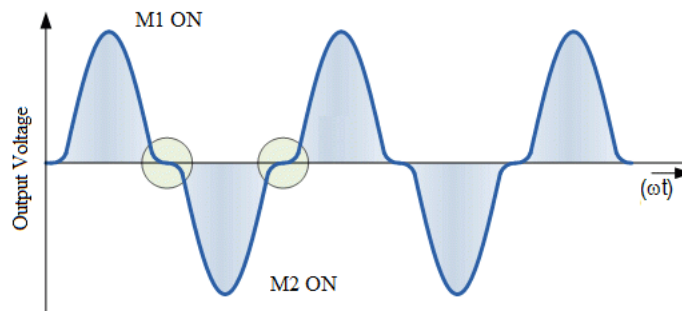


Figure 46. Crossover distortion for Class-B PA [125].

Between Class A and Class B amplifiers, there is another topology called Class AB. This class is a mix between both classes and presents a conduction angle between 180° and 360° . It will be discussed in Section 3.4.3.4.

3.4.3.3 Class C

Class C operates as previous classes but with a lower conduction angle and transistors working for less time. Theoretically, this class could reach 100% efficiency with a conduction angle of 0° . In practice this is not possible.

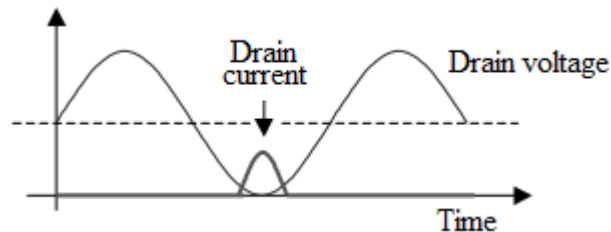


Figure 47. Drain voltage and current waveforms for Class-C [119].

When the conduction angle approaches 0 degrees, the output current also approaches zero [118], hence, the output power and gain decrease simultaneously. While Class A and Class B PAs are linear amplifiers, Class C PAs operate as nonlinear amplifiers. The output signal amplitude does not change linearly with respect to the input signal [5].

3.4.3.4 Class AB PA

Class AB amplifier results from biasing the transistor to operate between Class A and Class B. The transistor only conducts in less than a half of each of the driving cycles. It conducts between 180° and 360° . The amplifier is biased near the cutoff region with some continuous collector current flow. They are mainly used in push-pull amplifiers and can provide better linearity than Class B PA but with less efficiency [126].

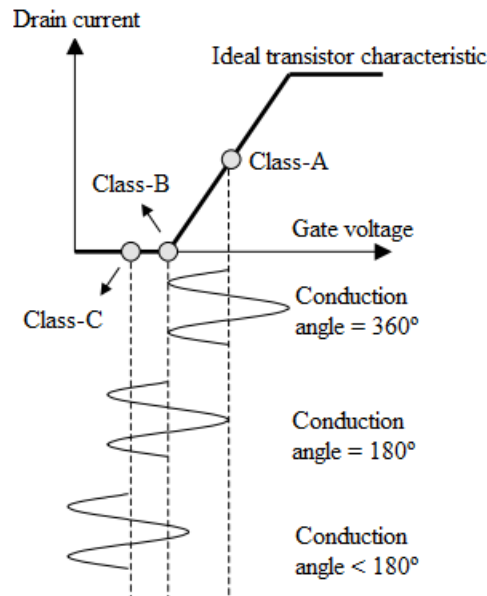


Figure 48. Conduction mode in different classes of amplification-mode PA [114].

As a summary, the conduction modes of different power amplifiers with ideal transistors are compiled in Figure 48. While the base voltage is a sinusoidal signal, the collector current varies depending on the class. In Class A, the transistor is always conducting with 2π conduction angle. In Class B, the transistor only conducts in half of the period, π conduction angle. In Class C, the transistor conducts less than half of the period, less than π conduction angle.

Topology	Angle of conduction	Maximum theoretical efficiency
Class A	360°	50%
Class B	180°	78.5%
Class C	180°-0°	78.5%-100%
Class AB	360°-180°	50%-78.5%

Table 7. Summary table of the theoretical characteristics of the amplification-mode PA.

3.4.4 Switching-mode PAs

Switching-mode power amplifiers came up with the idea of improving efficiency of amplifiers. The degradation of amplifier efficiency is due to the overlap of current and voltage in the transistor at the same time. Operating the transistor as a switch, it could be possible to achieve 100% efficiency [121]. This group involves D, E and F classes, plus some variations of them.

3.4.4.1 Class D

A Class D amplifier operates differently than the previous topologies. This class uses transistors as switches configured as inverters, shown in Figure 49. In this way, the voltage seen at the output varies between two voltage extremes. When one of the transistors conducts, the current which flows through it is high, but the voltage is considerable low. Thus, the power is only dissipated in the transition between ON and OFF. Similarly, when the transistor does not conduct, the voltage is high, but the current is low. Once again, there is no power dissipation except in state transitions. During the switching time, a short circuit from the supply to the ground could be generated. This problem can cause additional power dissipation and efficiency degradation. Due to this reason, designers must pay attention when designing the inverter of the power stage.

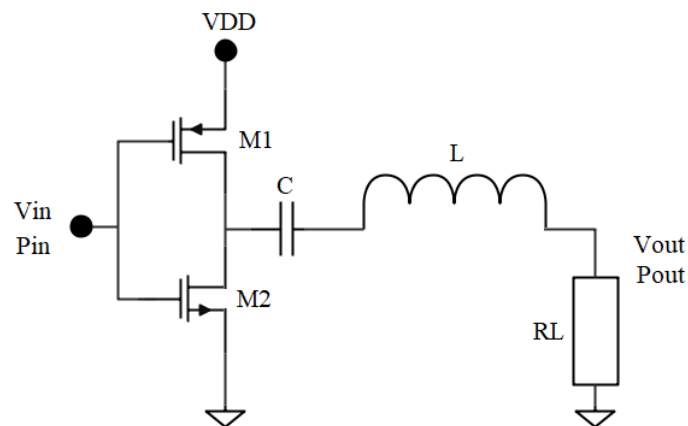


Figure 49. Class D PA [122].

Considering ideal switches, the output voltage is zero when the transistor is OFF, so no power dissipation is produced, and maximum efficiency of the power stage can reach 100%. In practice, this is not possible, as the transistors presents a non-zero on-resistance [117] and efficiency is reduced. The output seen after the transistors is a PWM signal. A filter is required after the power stage to reconvert the PWM signal into the sinusoidal signal that was received at the input [127].

3.4.4.2 Class E

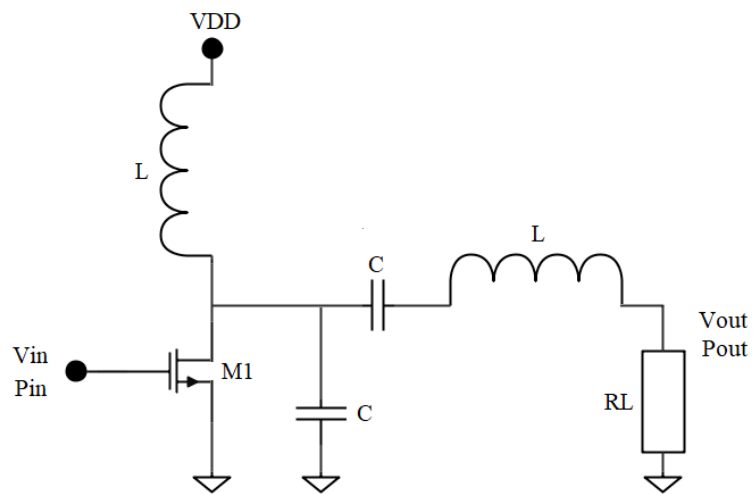


Figure 50. Class E PA [122].

Like Class D, Class E is also a switching amplifier. Main advantages with respect to the rest of the classes, are a high efficiency (being able to arrive theoretically at 100% like Class D), a higher reliability, reduced size and weight. This topology have shown better PAE performance in comparison with other classes due to its use of parasitic elements as part of the circuit [128].

As we have seen in previous topologies, the switch transition can become a considerable fraction of a signal period, especially in high-speed operation [129]. In that time, the voltage and current may be nonzero at same time, resulting in power dissipation. Class E power amplifiers are designed to minimize this loss.

3.4.4.3 Class F

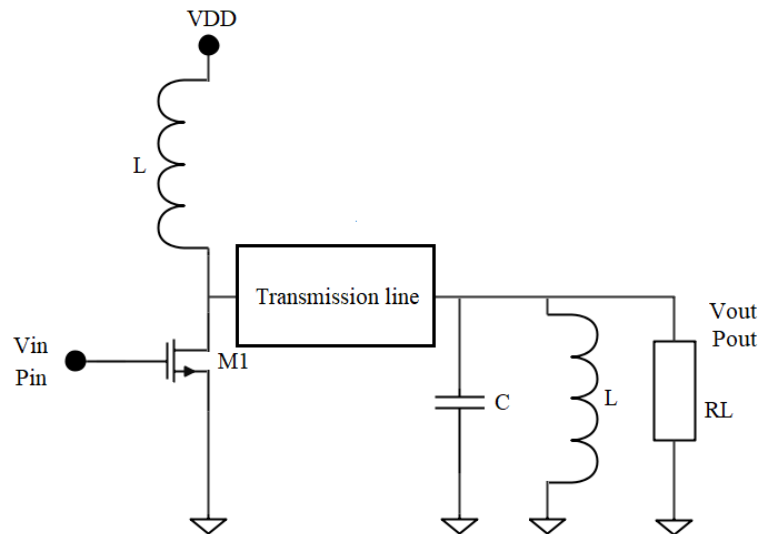


Figure 51. Class F PA [122].

Figure 51 above illustrates a Class F PA with a transmission line connected at the drain of the transistor. The Class F amplifier is one of the highest efficiency amplifiers. The transmission line consists on a tank which is tuned to resonate at the third harmonic. The quality factor of the resonator tank must be high enough to short circuit all frequencies outside the desired bandwidth [122]. The resonant output circuit is used to filter out all other harmonics, allowing only the fundamental frequency at the output.

3.4.5 Applications and Figure of Merits (FoMs)

As we said before, microwave PAs becomes an important issue in wireless communication systems, especially in fifth generation (5G) wireless services. They are used in the transmission part of the wireless communication systems and in automotive radar. For battery operated applications, minimum DC power consumption is required [121]. CMOS is the process chosen for recent power amplifier designs since they present low cost and high-level integration. On the other hand, this technology also has some drawbacks. CMOS processes provide less power efficiency than GaAs processes, due to limitations from substrate conductivity and silicon breakdown field. Hence, 5G wireless systems need efficient CMOS power amplifiers [130].

The International Terrestrial Reference System (ITRS) defined the power amplifier figure of merit (FoM_{PA}) in 2001. It considers the output power (P_{OUT}), the power gain (G), the power-added efficiency (PAE) and the carrier frequency (f). It is a standard to compare different power amplifier designs. However, linearity depends on the operating class of the amplifiers, which makes it difficult to compare different classes amplifiers.

$$FoM_{PA} = P_{OUT} \cdot G \cdot PAE \cdot f^2 \quad (22)$$

Despite of this, some authors have used other figure of merits to compare power amplifiers. One clear example is D. Zhao et al in [131]. The figure of merit they used is given by

$$FOM = P_{SAT}[dBm] + G[dB] + 20 \log(f_c[GHz]) + 10 \log(PAE_{MAX}[\%]) \quad (23)$$

Their 60 GHz power amplifier was implemented in 40 nm CMOS technology. It achieves 17 dB power gain and 30.3% PAE.

Reference	Architecture	CMOS Technology (nm)	Frequency (GHz)	Power Gain (dB)	P1dB (dBm)	Supply (V)	PAE (%)
[123]	4 Class A stages	65	58	13.4	12.2	1.2	7.6
[132]	2 Class AB stages	130	2.8-6	17.5	-*	1.2	36
[133]	Class AB	130	1.92	6	-*	1.2	26
[134]	2 Class C stages	130	2.4	25	22.7	3.2	60
[131]	2 Class AB stages	40	60	21.2	14	1.0	28.5
[131]	Class AB	40	60	17	13.8	1.0	30.3
[135]	Class AB	65	2-6	22.8-24.4	17.8-20.7	3.3	28.4
[136]	Class AB	180	3-7	14.5	7	1.8	-*
[137]	Class AB	180	2.4	31	-*	2.4	42
[138]	Class AB + Diode Linearization	250	2.4	11.2	20	2.5	28
[139]	Class AB	350	1.9	24.6	-*	2.5	35

**Missing information.*

Table 8. CMOS Amplification-Mode Power Amplifier comparison table.

Reference	Architecture	CMOS Technology (nm)	Frequency (GHz)	Pout (dBm)	Supply (V)	PAE (%)
[140]	Class D	130	1.85	32.0	-*	15.3
[141]	Differential Class E	130	1.6	30.5	2.5	48
[142]	Class F	130	3.5	20.5	1.8	52.9
[143]	Class D	28	1.8	32.4	-*	34.1
[144]	Inverse Class D	32	2.4	25.3	2	35
[145]	Class F	65	29	14.8	1.1	46.4
[146]	Inverse Class D	65	2.25	21.8	1	44
[147]	Class E + Class D	180	0.9	31.7	1.7-1.9	62.4
[128]	Class E + FB Technique	180	1.8	27.0	3.3	52
[148]	Class E	180	1.8	33.8	3.3	50
[149]	Class E	180	2.4	21.3	3.3	40
[150]	Class D	180	0.54	-*	-*	46
[129]	Differential Class E	350	2.0	-*	2	48

*Missing information.

Table 9. CMOS Switching-Mode Power Amplifier comparison table.

4. Conclusion

In this thesis, a compilation of general information about the components that form a receiver has been proposed. The device technology on which the low noise amplifiers, mixers, oscillators and power amplifiers shown in this thesis are based is CMOS with a 130 nm node process. However, a comparison with other designs using processes such 90, 180 or 250 nm, has also been carried out in order to compare the different performances.

5. References

- [1] J. Segura and C. F. Hawkins, “Mosfet Transistors,” in *CMOS Electronics: How It Works, How It Fails*, 2004, pp. 53-98.
- [2] R. Perret, “Power MOSFET Transistors,” in *Power Electronics Semiconductor Devices*, 2009, pp. 1-56.
- [3] B. Razavi, *Design of Analog CMOS Integrated Circuits*, McGraw-Hill, 2000.
- [4] ElProcus, “Electronic Projects Focus,” [Online]. Available: <https://www.elprocus.com/cmos-working-principle-and-applications/>. [Accessed May 2020].
- [5] C. Nguyen, *Radio-Frequency Integrated-Circuit Engineering*, New Jersey: John Wiley & Sons, 2015.
- [6] R. H. Yongwang Ding, “High-Linearity CMOS RF Front-End Circuits”.
- [7] M. S. Johan Janssens, “CMOS Cellular Receiver Front-Ends from Specification to Realization”.
- [8] F. Ellinger, *Radio Frequency Integrated Circuits and Technologies*, Dresden, Germany: Springer, 2007.
- [9] B. Zarlingo, “Keysight Technologies,” 30 May 2017. [Online]. Available: <https://community.keysight.com/community/keysight-blogs/rf-test/blog/2017/05/30/the-four-ws-of-noise-figure>. [Accessed April 2020].
- [10] “Everything RF,” 2 December 2018. [Online]. Available: <https://www.everythingrf.com/community/what-is-receiver-sensitivity>. [Accessed April 2020].
- [11] T. H. Lee and D. K. Shaeffer, “A 1.5-V, 1.5-GHz CMOS Low Noise Amplifier,” *IEEE Journal of Solid-State Circuits*, vol. 32, no. 5, pp. 745-759, 1997.
- [12] “What is physical significance of IP3, why it is more important in Receiver Chain ?,” Techplayon, 19 August 2017. [Online]. Available: <http://www.techplayon.com/physical-significance-iip3-important-receiver-chain/>. [Accessed April 2020].
- [13] S. J. Flores, “El receptor superheterodino,” Departamento de Comunicaciones. Universitat Politecnica de Valencia, 4 October 2017. [Online]. Available: <https://www.youtube.com/watch?v=f4qMdT6DmE0>. [Accessed April 2020].
- [14] L. Frenzel, “Chapter 9: Communication Receivers,” in *Principles of Electronic Communication Systems*, New York, USA, 2016, pp. 291-346.
- [15] C. Durdodt, A. Hanke, S. Heinen and U. Langmann, “Comparison of an inductorless low-IF and zero-IF receiver for Bluetooth,” *The 2002 45th Midwest Symposium on Circuits and Systems*, pp. 563-566, 2002.
- [16] B. M. Springer, “LNA Design in CMOS,” in *High-Linearity CMOS RF Front-End Circuits*, 2005.
- [17] T. Das, *Practical Considerations for Low Noise Amplifier Design*, May 2005.

- [18] S. Shekhar, J. S. Walling, S. Aniruddhan and D. J. Allstot, "CMOS VCO and LNA using tuned-input tuned-output circuits," in *IEEE Journal of Solid-State Circuits*, 2008.
- [19] T. Yao, M. Gordon, K. Yau, M. Yang and S. P. Voinigescu, "A 60-GHz PA and LNA in 90-nm RF-CMOS," *Proceedings of the IEEE Radio Frequency Integrated Circuits Symposium (RFIC)*, p. 4, 2006.
- [20] J. R. Long and D. J. Cassan, "A 1-V Transformer-Feedback Low-Noise Amplifier for 5-GHz Wireless LAN in 0.18- μ m CMOS," *IEEE Journal of Solid-State Circuits*, vol. 38, no. 3, 2003.
- [21] H. Song, H. Kim, K. Han, J. Choi, C. Park and B. Kim, "A sub-2 dB NF dual-band CMOS LNA for CDMA/WCDMA applications," *IEEE Microwave and Wireless Components Letters*, vol. 18, no. 3, pp. 212-214, 2008.
- [22] A. N. Karanicolas, "A 2.7V 900MHz CMOS LNA and mixer," *ISSCC Dig. Tech. Papers*, vol. 39, pp. 50-51, 1996.
- [23] A. Abidi, "On the operation of cascode gain stages," *IEEE Journal of Solid-State Circuits*, vol. 23, no. 6, pp. 1434-1437, 1988.
- [24] S. P. Voinigescu, T. O. Dickson, M. Gordon, C. Lee, T. Y. A. Mangan, K. Tang and K. H. K. Yau, *RF and millimeter-wave IC design in the nano-(Bi)CMOS era*, University of Toronto: Dept. of Electrical and Computer Engineering.
- [25] A. A. Abidi, "RF CMOS comes of age," *IEEE Journal of Solid-State Circuits*, vol. 39, no. 4, pp. 549-561, 2004.
- [26] E. Sánchez-Sinencio, X. Fan and H. Zhang, "A noise reduction and linearity improvement technique for a differential cascode LNA," *IEEE Journal of Solid-State Circuits*, vol. 43, no. 3, pp. 588-599, 2008.
- [27] W. Zhuo, S. H. K. Embabi and J. Pineda de Gyvez, "Using capacitive crosscoupling technique in RF low-noise amplifiers and down-conversion mixer design," *Proceedings of the European Solid-State Circuits Conference (ESSCIRC)*, pp. 116-199, 2000.
- [28] X. Li, S. Shekhar and D. J. Allstot, "Gm-booster common-gate LNA and differential Colpitts VCO/QVCO in 0.18- μ m CMOS," *IEEE Journal of Solid-State Circuits*, vol. 40, no. 12, pp. 2609-2619, 2005.
- [29] W. Zhuo, S. H. K. Embabi, J. Pineda de Gyvez and E. Sánchez-Sinencio, "A capacitor cross-coupled common-gate low noise amplifier," *IEEE Transaction on Circuits and Systems II: Express Briefs*, vol. 52, no. 12, pp. 875-879, 2005.
- [30] P. R. Gray, P. J. Hurst, S. H. Lewis and R. G. Meyer, *Analysis and Design of Analog Integrated Circuits*, New York: 4th Edition, 2001.
- [31] D. J. Allstot, X. Li and S. Shekhar, "Design considerations for CMOS low-noise amplifiers," *2004 IEEE Radio Frequency Integrated Circuits (RFIC) Systems. Digest of Papers*, pp. 97-100, 2004.
- [32] C. Andriesei and C. Turcă, "Revisiting the impedance matching for CS-LNA," *2017 International Symposium on Signals, Circuits and Systems (ISSCS)*, pp. 1-4, 2017.
- [33] B. Kim, D. Im, J. Choi and K. Lee, "A highly linear 1 GHz 1.3 dB NF CMOS low-noise amplifier with complementary transconductance linearization," *IEEE Journal of Solid-State Circuit*, vol. 49, no. 6, pp. 1286-1302, 2014.

- [34] F. Song, S. Tan and O. Shanaa, "An ultra-low-cost ESD-protected 0.65dB NF +10dBm OP1dB GNSS LNA in 0.18- μ m SOI CMOS," IEEE Asian Solid-State Circ. Conf. (A-SSCC), pp. 341-344, 2014.
- [35] E. Kargaran, G. Nabovati, M. Baghbanmanesh, K. Mafmezhad and H. Nabovati, "An ultra low voltage ultra high gain CMOS LNA using forward body biasing technique," IEEE International Midwest Symp. Circ. and Syst. (MWSCAS), pp. 1-4, 2011.
- [36] T. H. Lee, The design of CMOS radio-frequency integrated circuits, Cambridge University Press: 2nd Edition, 2004.
- [37] M. S. Paul Leroux, A 5 GHz CMOS Low-Noise Amplifier with Inductive ESD Protection Exceeding 3 kV HBM, Leuven, Belgium, 2004.
- [38] M. Vidojkovic, M. Sanduleanu, J. van der Tang, P. Baltus and A. van Roermund, A 1.2 V, Inductorless, Broadband LNA in 90 nm CMOS LP, Eindhoven, The Netherlands, 2007.
- [39] H. S. Savci, Z. Wang, A. Sula and N. S. Dogan, "A 1-V UHF low noise amplifier for ultralow-power applications," Proceedings of the IEEE International Symposium on Circuit and Systems (ISCAS2006), pp. 4495-4498, 2006.
- [40] L. Belostotski and J. Haslett, "Noise figure optimization of inductively degenerated CMOS LNAs with integrated gate inductors," IEEE Transactions on Circuits and Systems I: Regular Papers, vol. 53, no. 7, pp. 1409-1422, 2006.
- [41] A. Bevilacqua, A. Vallese, C. Sandner, M. Tiebout, A. Gerosa and A. Neviani, "A 0.13/ μ m CMOS LNA with Integrated Balun and Notch Filter for 3-to-5GHz UWB Receivers," 2007 IEEE International Solid-State Circuits Conference. Digest of Technical Papers, pp. 420-612, 2007.
- [42] F. Gianesello, D. Gloria, C. Raynaud and S. Boret, "5 GHz 1.4 dB NF CMOS LNA integrated in 130 nm High Resistivity SOI technology," 2007 International Symposium on Integrated Circuits, pp. 96-99, 2007.
- [43] S. Ambulker, J. Kumar Mishra and S. Nakhate, "A CMOS Low Noise Amplifier with Improved Gain," in Communications in Computer and Information Science, Springer, 2019, pp. 215-223.
- [44] T.-S. Kim and B.-S. Kim, "Post-linearization of cascode CMOS low noise amplifier using folded PMOS IMD sinker," IEEE Microwave and Wireless Components Letters, vol. 16, no. 4, pp. 182-184, 2006.
- [45] J. Sureja, S. Oza, Vineeta and P. Joshi, "An UWB CMOS LNA: Comparative Analysis of various LNA topologies," in National Conference on Power systems, Embedded Systems, Power electronics, Communication, Control and Instrumentation - PEPCCI, 2012.
- [46] A. Slimane, M. Trabelsi and M. Moussa, "Bandwidth improvement technique of distributed amplifiers using combined filtering structures," AEU - International Journal of Electronics and Communications, vol. 65, no. 10, pp. 777-782, 2011.
- [47] P. R. Kinget and F. Zhang, "Low-power programmable gain CMOS distributed LNA," IEEE Journal of Solid-State Circuits, vol. 41, no. 6, pp. 1333-1343, 2006.

- [48] S. O. Fateme Aghaee, "Distributed amplifier: a tutorial Review," in International Conference on Innovation, Knowledge and Enterprise, 2017.
- [49] C. Aitchison, "The intrinsic noise figure of the MESFET distributed," IEEE Trans. Microw. Theory Tech., vol. 33, no. 6, pp. 460-466, 1985.
- [50] Y.-W. Hsiao and M.-D. Ker, "An ESD-protected 5-GHz differential low-noise amplifier in a 130-nm CMOS process,," IEEE 2008 Custom Intergrated Circuits Conference (CICC), pp. 233-236, 2008.
- [51] C.-H. Liao and H.-R. Chuang, "A 5.7-GHz 0.18- μ m CMOS gain-controlled differential LNA with current reuse for WLAN receiver," IEEE Microwave and Wireless Components Letters, vol. 13, no. 12, pp. 526-528, 2003.
- [52] F. Gatta, E. Sacchi, F. Svelto, P. Vilmercati and R. Castello, "A 2-dB noise figure 900-MHz differential CMOS LNA," IEEE Journal of Solid-State Circuits, vol. 36, no. 10, pp. 1444-1452, 2001.
- [53] Q. Wan and C. Wang, "Design of 3.1–10.6 GHz ultra-wideband CMOS low noise amplifier with currentreuse technique," International Journal of Electronics and Communications (AEÜ), pp. 1006-1011, 2011.
- [54] J. Walling, S. Shekhar and D. Allstot, "A gm-Boosted Current-Reuse LNA in 0.18 μ m CMOS,," 2007 IEEE Radio Frequency Integrated Circuits (RFIC) Symposium, pp. 613-616, 2007.
- [55] T. Taris, J. Begueret and Y. Deval, "A low voltage current reuse LNA in a 130nm CMOS technology for UWB applications,," 2007 European Microwave Integrated Circuit Conference, pp. 307-310, 2007.
- [56] Y. Hsiao and M. Ker, "A 5-GHz Differential Low-Noise Amplifier With High Pin-to-Pin ESD Robustness in a 130-nm CMOS Process,," IEEE Transactions on Microwave Theory and Techniques, vol. 57, no. 5, pp. 1044-1053, 2009.
- [57] J. Borremans, S. Thijs, P. Wambacq, Y. Rolain, D. Linten and M. Kuijk, "A Fully Integrated 7.3 kV HBM ESD-Protected Transformer-Based 4.5–6 GHz CMOS LNA,," IEEE Journal of Solid-State Circuits, vol. 44, no. 2, pp. 344-353, 2009.
- [58] G. Dambrine and e. al, "High frequency low noise potentialities of down to 65nm technology nodes MOSFETs," IEEE GaAs Symposium, 2005.
- [59] A. Homayoun and B. Razavi, "A low-power CMOS receiver for 5 GHz WLAN,," IEEE J Solid-State Circuits 50, pp. 630-643, 2015.
- [60] M. Khurram and S. Hasan, "A 3–5 GHz Current-Reuse g_m -Boosted CG LNA for Ultrawideband in 130 nm CMOS,," IEEE Transactions on Very Large Scale Integration (VLSI) Systems, vol. 20, no. 3, pp. 400-409, 2012.
- [61] S. Asgaran, M. J. Deen and C.-H. Chen, "A 4-mW monolithic CMOS LNA at 5.7 GHz with the gate resistance used for input matching,," IEEE Microwave and Wireless Components Letters, vol. 16, no. 4, pp. 188-190, 2006.
- [62] H. Lee and S. Mohammadi, "A 3GHz sub-threshold CMOS low noise amplifier,," Proceedings of the IEEE Radio Frequency Integrated Circuits (RFIC) Symposium, 2006.
- [63] M. Sanduleanu, G. Zhang and J. Long, "31-34GHz low noise amplifier with on-chip microstrip lines and inter-stage matching in 90nm baseline CMOS,," Proceedings of the IEEE Radio Frequency Integrated Circuits (RFIC) Symposium, pp. 143-146, 2006.

- [64] O. Dupuis, X. Sun, G. Carchon, P. Soussan, M. Ferndahl, S. Decoutere and W. De Raedt, "24 GHz LNA in 90nm RF-CMOS with high-Q above-IC inductors,," Proceedings of the 31st European Solid-State Circuits Conference, pp. 89-92, 2005.
- [65] T. Liu, E. Westerwick, N. Rohani and R. Yan, "5-GHz CMOS radio transceiver front-end chipset,," IEEE Int. Solid-State Circuits (ISSCC) Dig. Tech. Papers, pp. 320-321, 2000.
- [66] M. Rafati, S. Qasemi, A. Nejati and P. Amiri, "A gm-Boosting 3–5 GHz Noise-Cancelling LNA,," 2019 27th Iranian Conference on Electrical Engineering (ICEE), pp. 376-379, 2019.
- [67] A. Vidhya and K. Suganthi, "A 5- GHz CMOS Low Noise Amplifier with High gain and Low power using Pre-distortion technique,," International Journal of Pure and Applied Mathematics, vol. 118, no. 20, pp. 4187-4194, 2018.
- [68] J.-H. Conan Zhan and S. Taylor, "A 5GHz resistive-feedback CMOS LNA for low-cost multi-standard applications,," 2006 IEEE International Solid State Circuits Conference - Digest of Technical Papers, pp. 721-730, 2006.
- [69] M. Lee and I. Kwon, "A 5-GHz highly linear floating-body CMOS LNA with switched gain control," Microwave and Optical Technology Letters, vol. 59, no. 3, pp. 593-596, 2017.
- [70] A. Madan, M. McPartlin, C. Masse, W. Vaillancourt and J. Cressler, "A 5 GHz 0.95 dB NF Highly Linear Cascode Floating-Body LNA in 180 nm SOI CMOS Technology,," IEEE Microwave and Wireless Components Letters, vol. 22, no. 4, pp. 200-202, 2012.
- [71] "Electronics Notes," [Online]. Available: <https://www.electronics-notes.com/articles/radio/rf-mixer/rf-mixing-basics.php#>. [Accessed April 2020].
- [72] D. K. Shaeffer and T. H. Lee, "CMOS Mixers," in The Design and Implementation of Low-Power CMOS Radio Receivers, Springer, Boston, MA, 2002, pp. 77-90.
- [73] "Arrow Electronics," [Online]. Available: <https://www.arrow.com/en/categories/rf-and-microwave/rf-ics/up-down-converters-and-mixers>. [Accessed 15 April 2020].
- [74] C. Nickolas, "The Basics of Mixers," October 2011. [Online]. Available: <https://www.digikey.com/en/articles/the-basics-of-mixers>. [Accessed April 2020].
- [75] R. Setty, D. Ji and H. Kaylie, "Figure of Merit of Mixer Intermod Performance," Mini-Circuits, 14 April 2015. [Online]. Available: <https://www.minicircuits.com/app/AN00-001.pdf>. [Accessed April 2020].
- [76] H. Walker, "Sources of intermodulation in diod-ring mixers,," The Radio and Electronic Engineer, vol. 46, no. 5, pp. 247-255, 1976.
- [77] "Electronics Notes," [Online]. Available: <https://www.electronics-notes.com/articles/radio/rf-mixer/gilbert-cell-rf-mixer.php>. [Accessed April 2020].
- [78] A. Kara-Omar, D. Dragomirescu, A. Coustou and R. Plana, "Low Power Ultra Wideband Up-Conversion Mixer in CMOS 0.13 um Technology," IEEE

- Mediterranean Electrotechnical Conference (MELECON 2010), pp. 1050-1055, 2010.
- [79] W.-S. Hxiao and Z.-M. Lin, "A 1-V 11.6-dBm IIP3 Up Conversion Mixer for UWB Wireless System," IEEE International Midwest Symposium on Circuits and Systems, pp. 1042-1046, 2009.
- [80] M. Rahman and R. Harjani, "A Sub-1-V 194- uW 31-dB FOM 2.3–2.5-GHz Mixer-First Receiver Frontend for WBAN With Mutual Noise Cancellation," IEEE Transactions on Microwave Theory and Techniques, vol. 64, no. 4, pp. 1102-1109, 2016.
- [81] H.-Y. Liao, C.-M. Tseng and H.-K. Chiou, "Lossy Lc Ladder Matching Network For Ultra-Wideband Cmos Gilbert Cell Mixer Design," Microwave And Optical Technology Letters, vol. 50, 2008.
- [82] W.-C. Wang, C.-P. Liao, Y.-K. Lo, Z.-D. Huang, F. R. Shahroury and C.-Y. Wu, "The Design of Integrated 3-GHz to 11-GHz CMOS Transmitter for Full-Band Ultra-Wideband (UWB) Applications," IEEE International Symposium on Circuits and Systems, pp. 2709-2712, 2008.
- [83] G. Sapone and G. Palmisano, "A 0.25- μ m CMOS Low-Power Up-Conversion Mixer for 3.1-5 GHz Ultra-Wideband Applications," 2006 Ph.D. Research in Microelectronics and Electronics, pp. 457-460, 2006.
- [84] R. Circa, D. Pienkowski and G. Boeck, "Integrated 130 nm CMOS passive mixer for 5 GHz WLAN applications," SBMO/IEEE MTT-S International Conference on Microwave and Optoelectronics, pp. 103-106, 2005.
- [85] A. Kara-Omar, D. Dragomirescu, A. Coustou and R. Plana, "UWB down-conversion mixer in CMOS 130 nm technology for wireless sensor network applied to aerospace application," 2013 European Microwave Integrated Circuit Conference, pp. 192-195, 2013.
- [86] G. Theodoratos, Y. Papananos and G. Vitzilaios, "A Low-Voltage 5-GHz Downconversion Mixer Employing A Second Harmonic Injection Linearization Technique," IEEE Transactions on Circuits and Systems II: Express Briefs, vol. 54, no. 11, pp. 964-968, 2007.
- [87] H.-. Wang, K.-. Wei, J.-. Lin and H.-. Chuang, "A 1.2-V low LO-power 3–5 GHz broadband CMOS folded-switching mixer for UWB receiver," 2008 IEEE Radio Frequency Integrated Circuits Symposium, pp. 621-624, 2008.
- [88] M.-F. Hung, C.-J. Kuo and S.-Y. Lee, "A 5.25-GHz CMOS folded-cascode even-harmonic mixer for-low voltage applications," IEEE Trans. Microw. Theory Tech., vol. 54, no. 2, pp. 660-669, 2006.
- [89] K.-H. Liang, H.-Y. Chang and Y.-J. Chan, "A 0.5–7.5 GHz Ultra Low-Voltage Low-Power Mixer Using Bulk-Injection Method by 0.18- μ m CMOS Technology," IEEE Microwave and wireless components letters, vol. 17, no. 7, pp. 531-533, 2007.
- [90] M. Abdelghany, R. Pokharel, H. Kanaya and K. Yoshida, "Low-voltage low-power combined LNA-single gate mixer for 5GHz wireless systems," 2011 IEEE Radio Frequency Integrated Circuits Symposium, pp. 1-4, 2011.
- [91] H. Hsieh and L. Lu, "Design of Ultra-Low-Voltage RF Frontends With Complementary Current-Reused Architectures," IEEE Transactions on Microwave Theory and Techniques, vol. 55, no. 7, pp. 1445-1458, 2007.

- [92] A. Safarian, A. Yazdi and P. Heydari, "Design and analysis of an ultrawide-band distributed CMOS mixer,," IEEE Transactions on Very Large Scale Integration (VLSI) Systems, vol. 13, no. 5, pp. 618-629, 2005.
- [93] X. Wang and R. Weber, "A novel low power low voltage LNA and mixer for WLAN IEEE 802.11a standard," Digest of Papers. 2004 Topical Meeting on Silicon Monolithic Integrated Circuits in RF Systems, pp. 231-234, 2004.
- [94] Y.-K. Chu, C.-H. Liao and H.-R. Chuang, "5.7 GHz 0.18 μm CMOS gain-controlled LNA and mixer for 802.11a WLAN applications," IEEE Radio Frequency Integrated Circuits (RFIC) Symposium, pp. 221-224, 2003.
- [95] M. Tiebout, "A Fully Integrated 51 GHz VCO in 0.13 μm CMOS," in Low Power VCO Design in CMOS, Springer, 2006, pp. 91-97.
- [96] M. Figueiredo and R. Aguiar, "Noise and Jitter in CMOS Digitally Controlled Delay Lines," 2006 13th IEEE International Conference on Electronics, Circuits and Systems, pp. 1356-1359, 2006.
- [97] I. Chlis, D. Pepe and D. Zito, "Analyses and techniques for phase noise reduction in CMOS Colpitts oscillator topology," International Journal of Circuit Theory and Applications, vol. 44, no. 3, pp. 616-638, 2015.
- [98] J. Jalil, M. Bin Ibne Reaz, M. Arif Sobhan Bhuiyan, L. Farzana Rahman and T. Gyu Chang , "Designing a Ring-VCO for RFID Transponders in 0.18 μm CMOS Process," The Scientific World Journal, 2014.
- [99] L. Rodoni, F. Ellinger and H. Jäckel, "CMOS inverter with 4.7 ps gate delay fabricated on 90 nm SOI technology," Electronics Letters, vol. 40, no. 20, pp. 1251-1252, 2004.
- [100] A. Mazzanti and P. Andreani, "Class-C Harmonic CMOS VCOs, With a General Result on Phase Noise," IEEE Journal of Solid-State Circuits, vol. 43, no. 12, pp. 2716-2729, 2008.
- [101] A. Aitoumeri, A. Bouyahyaoui and M. Alami, "5.18–7.42 GHz LC-VCO in subthreshold regime with low power low phase noise and immunity to PVT variations in 130 nm CMOS technology," Analog Integrated Circuits and Signal Processing, vol. 95, pp. 67-82, 2018.
- [102] J. Zhou, W. Li, D. Huang, C. Lian, N. Li, J. Ren and J. Chen, "A 0.4–6-GHz Frequency Synthesizer Using Dual-Mode VCO for Software-Defined Radio," IEEE Transactions on Microwave Theory and Techniques, vol. 61, no. 2, pp. 949-859, 2013.
- [103] A. Bevilacqua, F. P. Pavan, C. Sandner, A. Gerosa and A. Neviani, "Transformer-Based Dual-Mode Voltage-Controlled Oscillators," IEEE Transactions on Circuits and Systems II: Express Briefs, vol. 54, no. 4, pp. 293-297, 2007.
- [104] M. Mehrabian, A. Nabavi and N. Rashidi, "A 4~7GHz ultra wideband VCO with tunable active inductor," 2008 IEEE International Conference on Ultra-Wideband, pp. 21-24, 2008.
- [105] Y. J. Lee and C. S. Kim, "Q - Enhanced 5GHz CMOS VCO Using 4-port Transformer," 2007 Topical Meeting on Silicon Monolithic Integrated Circuits in RF Systems, pp. 119-122, 2007.
- [106] F. Farhabakhshian, T. Brown, K. Mayaram and T. Fiez, "A 475 mV, 4.9 GHz enhanced swing differential Colpitts VCO in 130 nm CMOS with an FoM of

- 196.2 dBc/Hz,” IEEE Custom Integrated Circuits Conference 2010, pp. 1-4, 2010.
- [107] J.-h. Duan, J.-p. Li and C. Qin, “A 2.5GHz Low Phase Noise LC VCO for WLAN Applications in 0.18 μm CMOS Technology,” 3rd IEEE International Symposium on Microwave, Antenna, Propagation and EMC Technologies for Wireless Communications, 2009.
- [108] K. Kwok and H. Luong, “Ultra-low-Voltage high-performance CMOS VCOs using transformer feedback,” IEEE Journal of Solid-State Circuits, vol. 40, no. 3, pp. 652-660, 2005.
- [109] Z. Li and K. K. O, “A low-phase-noise and low-power multiband CMOS voltage-controlled oscillator,” IEEE Journal of Solid-State Circuits, vol. 40, no. 6, pp. 1296-1302, 2005.
- [110] T. Huang and Y. Tseng, “A 1 V 2.2 mW 7 GHz CMOS Quadrature VCO Using Current-Reuse and Cross-Coupled Transformer-Feedback Technology,” IEEE Microwave and Wireless Components Letters, vol. 18, no. 10, pp. 698-700, 2008.
- [111] J. Hou and Y. Wang, “A 5 GHz Differential Colpitts CMOS VCO Using the Bottom PMOS Cross-Coupled Current Source,” IEEE Microwave and Wireless Components Letters, vol. 19, no. 6, pp. 401-403, 2009.
- [112] M. Tiebout, “A Fully Integrated 1.3 GHz VCO for GSM in 0.25 μm Standard CMOS with a Phase Noise of -142 dBc/Hz at 3 MHz Offset,” Proc. of the 30th European Microwave Conference, 2000.
- [113] M. Tiebout, “1.8 GHz Quadrature VCO Design for DCS1800 and GSM,” in Low Power VCO Design in CMOS, Springer, 2006, pp. 83-90.
- [114] R.-C. Liu, H.-Y. Chang, C.-H. Wang and H. Wang, “A 63 GHz VCO using a standard 0.25 μm CMOS process,” 2004 IEEE International Solid-State Circuits Conference (IEEE Cat. No.04CH37519), vol. 1, pp. 446-447, 2004.
- [115] S. Kousai, K. Onizuka, S. Hu, H. Wang and A. Hajimiri, “A new wave of CMOS power amplifier innovations: Fusing digital and analog techniques with large signal RF operations,” Proceedings of the IEEE 2014 Custom Integrated Circuits Conference, pp. 1-8, 2014.
- [116] I. Aoki, S. Kee, D. Rutledge and A. Hajimiri, “Distributed active transformer-a new power-combining and impedance-transformation technique,” IEEE TMTT, vol. 50, no. 1, pp. 316-331, 2002.
- [117] R. S. Narayanaswami, “RF CMOS Class C Power Amplifiers for Wireless Communications,” University of California, Berkeley, 2001.
- [118] N. Wongkomet, Efficiency Enhancement Techniques for CMOS RF Power Amplifiers, University of California at Berkeley: Ph.D. Thesis, Technical Report No. UCB/EECS-2006-74, 2006.
- [119] V. Prodanov and M. Banu, “Power amplifier principles and modern design,” in Wireless Technologies, Systems, Circuits Devices, K. Iniewski, Ed., 2008, pp. 349-381.
- [120] I. Keysight Technologies. [Online]. Available: http://rfmw.em.keysight.com/wireless/helpfiles/89600b/webhelp/subsystems/digdemod/Content/digdemod_syntblerrdata_evm.htm. [Accessed May 2020].

- [121] A. Mukherjee, "High-frequency benchmark circuits for compact model verification with special emphasis on evaluating the impact of physical effects on circuit performance," Dissertation, CEDIC, 2017.
- [122] J. Fritzin, *Power Amplifier Circuits in CMOS technologies*, Department of Electrical Engineering Linköpings universitet, SE-581 83 Linköping, Sweden, 2009.
- [123] T. Quémerais, L. Moquillon, S. Pruvost, J.-. Fournier, P. Benech and N. Corrao, "A CMOS class-A 65nm power amplifier for 60 GHz applications," 2010 Topical Meeting on Silicon Monolithic Integrated Circuits in RF Systems (SiRF), pp. 120-123, 2010.
- [124] A. Beohar and D. Baghel, "A Class AB Amplifier with a Reduced Crossover Distortion for Real Time Video Applications," *International Journal of Engineering Science and Technology*, vol. 2, no. 7, pp. 2783-2789, 2010.
- [125] "Electronics Tutorials," [Online]. Available: https://www.electronicstutorials.ws/amplifier/amp_7.html. [Accessed May 2020].
- [126] L. Frenzel, "Chapter 8: Radio Transmitters," in *Electronic Communication Systems*, New York, USA, 2016, pp. 236-290.
- [127] A. Pini, "DigiKey," 31 October 2018. [Online]. Available: <https://www.digikey.com/es/articles/simplify-portable-low-power-audio-circuit-design-class-d-amplifiers>. [Accessed May 2020].
- [128] A. Dehqan, S. Toofan and H. Lotfi, "Floating Bulk Cascode Class-E Power Amplifier," *IEEE Transactions on Circuits and Systems II: Express Briefs*, vol. 66, no. 4, pp. 537-541, 2019.
- [129] K.-C. Tsai and P. R. Gray, "A 1.9-GHz, 1-W CMOS class-E power amplifier for wireless communications," *IEEE Journal of Solid-State Circuits*, vol. 34, no. 7, pp. 962-970, 1999.
- [130] S. Shakib, H. Park, J. Dunworth, V. Aparin and K. Entesari, "A Highly Efficient and Linear Power Amplifier for 28-GHz 5G Phased Array Radios in 28-nm CMOS," *IEEE Journal of Solid-State Circuits*, vol. 51, no. 12, pp. 3020-3036, 2016.
- [131] D. Zhao and P. Reynaert, "A 60-GHz Dual-Mode Class AB Power Amplifier in 40-nm CMOS," *IEEE Journal of Solid-State Circuits*, vol. 48, no. 10, pp. 2323-2337, 2013.
- [132] A. Basaligheh, P. Saffari, M. Taherzadeh-Sani and F. Nabki, "A Highly Efficient and Linear Broadband Common-Drain CMOS Power Amplifier With Transformer-Based Input-Matching Network," *IEEE Microwave and Wireless Components Letters*, vol. 25, no. 12, pp. 814-816, 2015.
- [133] Y. Chee, J. Rabaey and A. Niknejad, "A class A/B low power amplifier for wireless sensor networks," 2004 IEEE International Symposium on Circuits and Systems (IEEE Cat. No.04CH37512), pp. IV-409, 2004.
- [134] J. Kang, D. Yu, K. Min and B. Kim, "A Ultra-High PAE Doherty Amplifier Based on 0.13um CMOS Process," *IEEE Microwave and Wireless Components Letters*, vol. 16, no. 9, pp. 505-507, 2006.
- [135] W. Ye, K. Ma and K. Yeo, "2.5 A 2-to-6GHz Class-AB power amplifier with 28.4% PAE in 65nm CMOS supporting 256QAM," 2015 IEEE International

- Solid-State Circuits Conference - (ISSCC) Digest of Technical Papers, pp. 1-3, 2015.
- [136] S. Murad, R. Pokharel, A. Galal, R. Sapawi, H. Kanaya and K. Yoshida, "An Excellent Gain Flatness 3.0–7.0 GHz CMOS PA for UWB Applications," *IEEE Microwave and Wireless Components Letters*, vol. 20, no. 9, pp. 510-512, 2010.
- [137] T. Sowlati and D. Leenaerts, "A 2.4 GHz 0.18 μm CMOS self-biased cascode power amplifier with 23 dBm output power," 2002 IEEE International Solid-State Circuits Conference. Digest of Technical Papers (Cat. No.02CH37315), vol. 1, pp. 294-467, 2002.
- [138] C.-C. Yen and H.-R. Chuang, "A 0.25- μm 20-dBm 2.4-GHz CMOS power amplifier with an integrated diode linearizer," *IEEE Microwave and Wireless Components Letters*, vol. 13, no. 2, pp. 45-47, 2003.
- [139] A. Giry, J.-. Fourniert and M. Pons, "1.9 GHz low voltage CMOS power amplifier for medium power RF applications," 2000 IEEE Radio Frequency Integrated Circuits (RFIC) Symposium Digest of Papers (Cat. No.00CH37096), pp. 121-124, 2000.
- [140] J. Fritzin, C. Svensson and A. Alvandpour, "A +32 dBm 1.85 GHz class-D outphasing RF PA in 130nm CMOS for WCDMA/LTE," 2011 Proceedings of the ESSCIRC (ESSCIRC), pp. 127-130, 2011.
- [141] R. Brama, L. Larcher, A. Mazzanti and F. Svelto, "A 30.5 dBm 48% PAE CMOS class-E PA with integrated balun for RF applications," *IEEE J. Solid-State Circuits*, vol. 43, no. 8, pp. 1755-1762, 2008.
- [142] Y. Sun and S. Du, "A 20.5 dBm Outphasing Class-F PA with Chireix Architecture at 3.5 GHz for RF Transmitter Front-end Architecture at 3.5 GHz for RF Transmitter Front-end," *IOP Conf. Series: Materials Science and Engineering*, vol. 717, 2020.
- [143] M. Martelius, K. Stadius, J. Lemberg, T. Nieminen, E. Roverato, M. Kosunen and J. Ryyänen, "Class D CMOS power amplifier with on/off logic for a multilevel outphasing transmitter," 2016 IEEE International Symposium on Circuits and Systems (ISCAS), pp. 710-713, 2016.
- [144] H. Xu, Y. Palaskas, A. Ravi, M. Sajadieh, M. El-Tanani and K. Soumyanath, "A Flip-Chip-Packaged 25.3 dBm Class-D Outphasing Power Amplifier in 32 nm CMOS for WLAN Application," *IEEE Journal of Solid-State Circuits*, vol. 46, no. 7, pp. 1596-1605, 2011.
- [145] S. Ali, P. Agarwal, S. Gopal, S. Mirabbasi and D. Heo, "A 25–35 GHz Neutralized Continuous Class-F CMOS Power Amplifier for 5G Mobile Communications Achieving 26% Modulation PAE at 1.5 Gb/s and 46.4% Peak PAE," *IEEE Transactions on Circuits and Systems I: Regular Papers*, vol. 66, no. 2, pp. 834-847, 2019.
- [146] D. Chowdhury, S. Thyagarajan, L. Ye, E. Alon and A. Niknejad, "A Fully-Integrated Efficient CMOS Inverse Class-D Power Amplifier for Digital Polar Transmitters," *IEEE Journal of Solid-State Circuits*, vol. 47, no. 5, pp. 1113-1122, 2012.
- [147] J. Jang, C. Park, H. Kim and S. Hong, "A CMOS RF Power Amplifier Using an Off-Chip Transmission Line Transformer With 62% PAE," *IEEE*

- Microwave and Wireless Components Letters, vol. 17, no. 5, pp. 385-387, 2007.
- [148] H. Lee, C. Park and S. Hong, "A Quasi-Four-Pair Class-E CMOS RF Power Amplifier With an Integrated Passive Device Transformer," IEEE Transactions on Microwave Theory and Techniques, vol. 57, no. 4, pp. 752-759, 2009.
- [149] V. Saari, P. Juurakko, J. Ryyanen and K. Halonen, "Integrated 2.4 GHz class-E CMOS power amplifier," 2005 IEEE Radio Frequency integrated Circuits (RFIC) Symposium - Digest of Papers, pp. 645-648, 2005.
- [150] J. Hur, O. Lee, C. Lee, K. Lim and J. Laskar, "A Multi-Level and Multi-Band Class-D CMOS Power Amplifier for the LINC System in the Cognitive Radio Application," IEEE Microwave and Wireless Components Letters, vol. 20, no. 6, pp. 352-354, 2010.
- [151] C.-W. Kim, M. Jung and S. Lee, "Ultra-Wideband CMOS low noise amplifier," Electronics letters, vol. 41, no. 7, pp. 384-385.

All websites and online documents were last accessed in June 2020.

